Innovation of Chemistry & Materials for Sustainability

Volume 1, Issue 1, Jul-Dec **2024**

REVIEW ARTICLE

ISSN (Print): 3049 – 2548
ISSN (Online): 3049 – 0146

Recent Development and Challenges in Metal Chalcogenide Quantum Dots: From Material Design Strategies to Applications

Pratibha Chahal, Aayushi Goel and Avinash Singh*

Department of Chemistry, SRM University Delhi-NCR, Sonipat-131029, Haryana, India
*Correspondence: avinash.s@srmuniversity.ac.in

Abstract: Nanotechnology advancements in recent times have led to the development of various metal chalcogenide quantum dots (QDs), including binary QDs (metal sulfide, selenide, and telluride) and alloyed QDs (cadmium selenium telluride). These QDs are valued for their distinctive optoelectronic and functional properties, including intrinsic (quantum confinement) and extrinsic (high surface area) effects influenced by size, shape, and surface characteristics. This review article mainly focuses on the most recent advancements in the synthesis, properties, and applications of metal chalcogenide QDs. We cover different synthesis approaches, including solvothermal, wet chemical, aqueous, photochemical, mechanochemical, and green synthesis, and explain how these techniques impact their properties. We then examine the diverse applications of QDs, including LEDs, biomedical, photovoltaics, neuromorphic, photodetector, photocatalysis, and sensing. Lastly, we explore the challenges and future opportunities for metal chalcogenide quantum dots. This article will provide a deeper understanding of the metal chalcogenide QDs. Moreover, it is beneficial for the researchers to make efficient QDs with various applications.

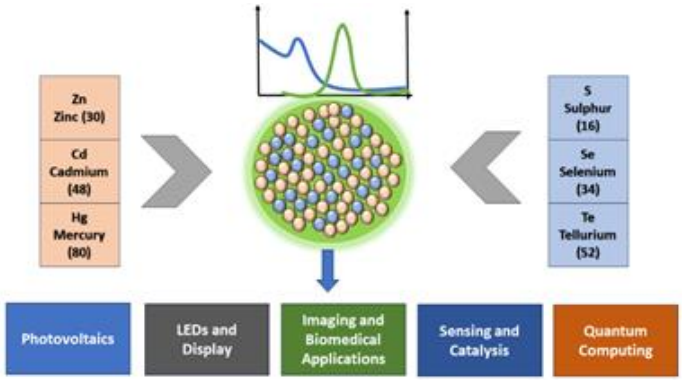

Keywords: *chalcogenide, QDs, quantum confinement, synthesis, properties, applications.*

Contents

1. Introduction

Modern, multidisciplinary nanotechnology has arisen from the development and research with inorganic nanomaterials which include metal, metal oxide, and semiconductor nanoparticles.[1]

Quantum Dots (QDs) were first discovered by the Russian scientist Alexey Ekimov in 1981 in a glass matrix while he was employed at the Vavilov State Optical Institute in St. Petersburg.[2] However, it was Louis Brus, a semiconductor researcher at AT&T Bell Laboratories in New Jersey, who found the first colloidal solutions of QDs.[2] Brus referred to QDs as "small semiconductor crystallites". Later Moungi Bawendi and coworkers worked extensively to synthesize CdS, CdSe, and other chalcogenide QDs in the upcoming years.[3] For their contribution to the discovery and synthesis of QDs, Alexey Ekimov, Louis Brus and Moungi Bawendi were awarded the Nobel Prize in chemistry in 2023.

Pratibha Chahal received her master's degree in chemistry with a specialization in physical chemistry from Maharshi Dayanand University, Rohtak in 2020. She qualified Net JRF (2022), HTET (2022), and CTET (2023). At present, she pursuing PhD from SRM University, Delhi-NCR, Sonipat under the guidance of Dr. Avinash Singh. Her research interest lies in semiconductor QDs and nanotechnology.

Aayushi Goel is from Samalkha, Haryana, India. She completed her BSc in Chemistry from Kurukshetra University, Kurukshetra, Haryana and is pursuing MSc Chemistry (2024) from SRM University, Delhi-NCR, Sonepat. Her research interest is in nanotechnology and material science.

Dr. Avinash Singh studied BSc (Hons), Chemistry and MSc, Chemistry from Banaras Hindu University, and obtained his PhD from Radiation & Photochemistry Division, Bhabha Atomic Research Centre (BARC), Mumbai, India in 2018. Currently, he is serving as Assistant Professor in the Department of Chemistry, SRM University Delhi-NCR, Sonepat. His research interest lies in semiconductor nanomaterials, radiation chemistry and photochemistry.

In the past few years, semiconductor metal chalcogen based QDs have attracted wide interest in bioimaging and biomedical industries due to their good optoelectronic properties.[4] QDs are semiconductor nanocrystals that are small enough to display size-dependent characteristics and come in the range of 1-10 nm.[4] These are zero-dimensional nanomaterials, the terms "quantum" and "dot" imply that the particles—electrons, which transfer electricity—are restricted and have well-defined energy levels.[5] They are restricted in all three spatial directions[6] due to which these nanocrystals are also referred to as "low-dimensional" quantum structures.[7,8]

Most of the QDs are made from the combination of metal (group I and II) and chalcogens (group VI).[9] Chalcogens are the elements in the periodic table that belong to group VI elements including oxygen, sulfur (S), selenium (Se),

http://doi.org/10.63654/icms.2024.01030
Received: 30 May 2024; Revised: 23 July 2024; Accepted: 07 September 2024; Published (online): 28 October 2024

tellurium (Te), and polonium (Po).[10] Out of these, the metal oxide is not considered chalcogenide as these oxides have different chemical properties in comparison to sulphide, selenide, and telluride[11]. The common chalcogens which are used in the preparation of QDs are sulphur, selenium, and tellurium[12]. Po is highly radioactive hence it is not used in the synthesis of QDs. The synthesis of semiconductor NCs in an aqueous medium primarily relies on Lewis's acid/base reactions, which invariably involve H^+, OH^-, and H_2O. A chemical species that gives away an electron pair is called a Lewis base, and the one that accepts a base's electron pair is termed a Lewis acid.[13] These are further divided based on of their polarizability by the HSAB concept (Hard and soft acids and bases). "Soft" species are large in size, low-charge and weakly polarizable are "Hard" species. However, they are relatively small, and high-charge.[13] This is the one of important concepts for the understanding of solubility of various kinds of compounds. Chalcogen ions like S^{2-}, Se^{2-}, and Te^{2-} are considered soft bases, whereas transition metal ions, based on their oxidation state, can be "soft" acids[13] like Cd^{2+}, or "borderline" acids, such as Pb^{2+} and Zn^{2+}. According to the HSAB principle, chalcogens easily make insoluble compounds with the most of transition metal ions in water because of the poor solubility of their products. When compared with solids created by hard−hard interactions, the bonds in soft−soft interactions are stronger, which provides transition metal chalcogenides with their semiconducting properties.[13] We can modify the size and composition, to obtain luminescence across the entire spectrum i.e. from UV to IR.[13] The colloidal technique, which precipitates semiconductor crystals from a solution, yields the smallest structures.[14]

QDs are classified into different categories: binary, ternary or quaternary[15] based on their composition. A binary QD has two elements (most commonly one metal from group II (Zn, Cd, Hg) and one chalcogen). Similarly, ternary, and quaternary QDs consist of three and four elements respectively. Examples of some most widely used binary QDs are ZnS, CdS, CdSe, etc. ZnCdS, ZnCdSe, are CuInS are examples of ternary QDs. Copper Zinc Tin Selenide (CZTS) is an example of quaternary QDs. Chemically and structurally, ternary I-III-VI and binary II-VI semiconductors differ from one another. PbS, CdS, or InAs are examples of binary semiconductor compounds that can be used to create binary QDs, which are semiconductor crystals at the nanoscale size.[16] Ternary QDs composed of group I-III-VI elements exhibit lower toxicity and radiation stability elements which sparked increased interest in their application to cancer treatment.[17] The term "artificial atoms"[18] is frequently used to describe them since they can be made to resemble actual atoms in terms of their discrete electronic energy levels and electronic wave functions.[19]

One of the most extensive studies of chalcogenide based QDs is of II-VI semiconductors. Cadmium selenide (CdSe) is among the most significant semiconductors that have a size less than the Bohr radius of exciton (5.7 nm)[20] with a moderate band gap (Eg) of 1.75 eV at 300 K.[21] CdSe QDs are highly luminescent, fluorescent and have better quantum yield with flexible processability.[22] It was possible to create and analyze a CdSe QDs sensitized solar cell (QDSSC). It is possible to create QDs that have the potential to both absorb and emit light across the whole solar spectrum.[22]

Saad *et al.*[23] reported the formation of CdSe QDs attached with chosen metal phthalocyanine (MPc) (like ZnPc and CuPc), employing the hot-injection organometallic approach. The resulting QDs exhibit same particle size and spherical morphology. They found CdSe QDs show clear photoluminescence (PL) peak of shorter wavelength.[23] QDs have the capacity for sensing as have proven beneficial in different specific applications, such as medicine and optoelectronics. Their intrinsic photostability, long fluorescence lifetime, and excitation wavelength far from the emission are the key justifications for their application in medicine.[24]

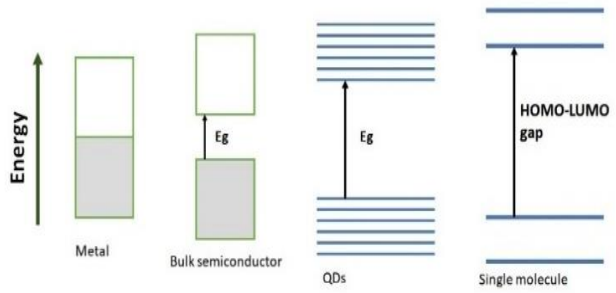

Figure 1: *The band structure from metal to bulk semiconductor to QDs and molecules.*

1.1 Properties

QDs and bulk materials differ in certain ways.[24,25] Bulk materials are bigger whereas QDs are so small, they have a large surface-to-volume ratio, results in QDs exhibit a high degree of reactivity. In contrast, bulk materials are significantly large. Unlike, bulk materials, which present a continuous range of energy levels, QDs feature discrete quantized energy levels shown as delta-like function in the density of states[23,24] demonstrated in figure 2. The smallest QDs can be achieved using the colloidal technique, where semiconductor crystals are precipitated out of a solution[26]. Temperature is an essential component in the synthesis process, and using high boiling point solvents helps to maintain controlled reactions.[26] Nanocrystallites, can exhibit optical, electronic, and structural characteristics that are frequently absent from both isolated molecules and macroscopic solids.[27] Nanocrystallites of semiconductors have specific electronic transitions that are tunable with size[28]. They can be highly polarizable when they are excited, making them useful for optoelectronic applications.[28] Lia *et al.*[29] reported suitable applications of ZnS QDs that optical properties can be changed based on their size due to quantum size effect. As discussed QDs have size in nanometer scale, and are made up of element from groups II to VI or III to V, which have dimensions smaller than the Bohr exciton radius.[30,31]

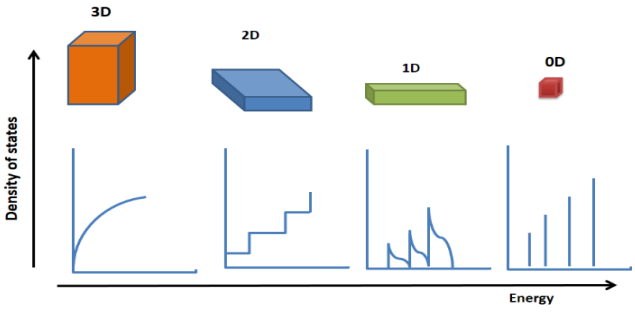

Figure 2: *Variation of density of states for 3D, 2D, 1D and 0D materials*

Quantum Confinement Effect: Another important effect which describes the particle size i.e. Quantum confinement effect. Quantum confinement effects elucidate the behavior of electrons through the use of energy levels, potential holes, electron energy bands, valence bands, and conduction bands. This phenomenon is observed when the particle size is significantly smaller than electron's wavelength consequently, the band gap energy increases as the QDs diameter decreases. As a result, both the absorption and emission spectral band edges of the QDs shift to shorter wavelengths as the particle size decreases, showing significant size dependence.[32] Andersen *et al.*[33] reported that quantum confinement effect creates the energy levels further a part as the particles size reduced. They study various

features due to the varying size limits on each energy level. One significant effect of quantum confinement in CdSe semiconductor QDs is that rises in the band gap with decreasing QD size. Since this is observed as a rise in the lowest exciton peak's energy as the QD's radius decreased.[33]

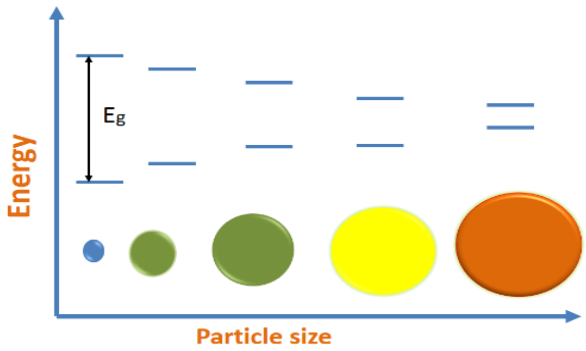

Figure 3: *Variation in band gap with the size of the QDs as a consequence of quantum confinement effect.*

Size-dependent: The optical properties of metal chalcogenide QDs depends upon shape and size of the QDs. Smaller particle size leads to a larger band gap hence the excitonic peak position is towards the smaller wavelength which keep on increasing upon increasing in particle size.[34] A small and uniform sized QD have a clear excitonic peak and a sharp emission profile. A color change from pale green to pale orange and finally to red with increasing temperature, showing a rise in particle size from Oswald ripening[34] (fig. 3). Because of their small size, QD electrons are trapped in a small space, even when their sizes are smaller than the exciton Bohr radius.[35] This implies that a significant energy level splitting occurs after an electron and a hole separate in an electron-hole pair.[35]

The Bohr exciton radius refers to the distance in the model of the exciton pair (electron-hole pair). In bulk, the size exceeds the Bohr radius (figure 4). hence the quantum confinement effect is not observed. However, upon reduction in size below the Bohr radius (in the nano region) the energy level of the semiconductor becomes discrete due to confinement of exciton pair which is described as the quantum confinement effect.

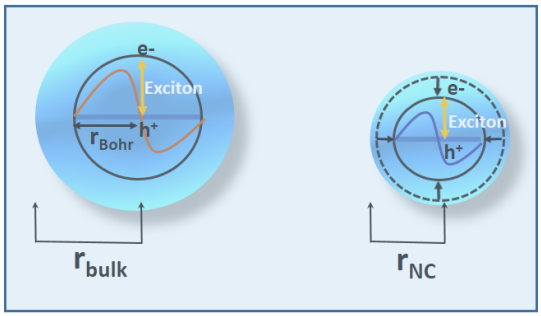

Figure 4: *The Bohr radius in the bulk and nanocrystals*

The band gap calculated by the Tauc equation (equation 1) and the particle size calculated by the Brus equation (equation 2) provides an estimate of the particle size.[36]
The band gap calculated by the Tauc equation (equation 1) is given below:
Tauc equation:

$$(\alpha h\nu) = B(h\nu - E_g)^r \qquad (1)$$

B = constant, r is the index which depends on nature of the electronic transition (r = ½ for direct band gap semiconductor and r = 2 for indirect band gap semiconductor).

α = absorption coefficient
hν is the photon energy
E_g = optical band gap
Tauc equation is used to calculate optical transition energy.

Using CdS and CdSe as examples, Brus (1984) provided the first theoretical calculation for a spherical semiconductor colloidal nanocrystal based on effective mass approximation.[37] The band gap energy in Brus's calculation is

$$\Delta E(r) = E_g + [h^2/8r^2(1/m^8_e + 1/m^8_h)] \qquad (2)$$

E_g= bulk band gap
h= Planck's constant, r= radius of QD
m_e is the mass of electron, m_h is the mass of electron hole

Apart from these two equations Scherrer equation can also be employed for the determination of mean size of particle using the XRD pattern. The Scherrer equation (equation 3)

$$D = K\lambda/\beta\cos\theta \qquad (3)$$

K is the Scherrer constant, λ is wavelength of the X-ray beam, β is the Full width at half maximum (FWHM) of the peak, θ is the Bragg angle.
The Scherrer constant, whose value is typically taken to be 0.9, indicates the particle's form[38]. To determine the crystal grain size, the Scherrer equation utilizes the width of the largest XRD peak for a specific sample.[38]

Composition of the QDs: The optical properties of the QDs is also governed with the composition of the QDs. A bulk semiconductor having smaller size metal ions and chalcogenide ions have large band gap and a semiconductor having bigger size metal ions and chalcogenide ions have small band gap. For example- the band gap of ZnS, ZnSe and ZnTe are 3.97, 3.10 and 2.26 eV respectively. Similarly, bulk CdS, CdSe and CdTe have band gaps of 2.4, 1.74, and 1.49 eV respectively.

Surface to volume ratio: It is well established that the melting temperature of nanoparticles decreases as the surface-to-volume ratio increases. The shape also has a prominent role in determining the surface-to-volume ratio of the particles.[39] The shape factor compares the contact regions of spherical nanoparticles with non-spherical particles that have the same volume.[40] It is serves for account the shape difference, especially in polyhedral nanoparticles.[40]
The simplest QDs are binary which are synthesized using one metal precursor and a chalcogenide. Zinc sulfide (ZnS), identified as II-VI binary compound, particular corresponding to a band gap of 4.49 eV.[41] In addition, ZnS QDs are non-toxic and have good chemical stability than various semiconductor QDs. As a result, ZnS QDs are well-suited for use in electroluminescent devices, light emitting diodes (LEDs), flat-panel displays, sensors, optoelectronic devices and photocatalysis in water purification.[41]
The another binary QD *i.e.* Cadmium selenide NCs display a range of colors and luminescence, with smaller crystal sizes corresponding to higher energy transitions.[30,42]

2. Synthesis of Chalcogenide QDs

Binary QDs are synthesized using one metal precursor and a chalcogenide. Li *et al.*[41] adeptly formulated using a controlled solvothermal synthesis approach with a size of not more than 3 nm. The method is much easier for controlling size than the other traditional methods. Also, the absorption and luminescence showed new characteristics which may be caused by the quantum

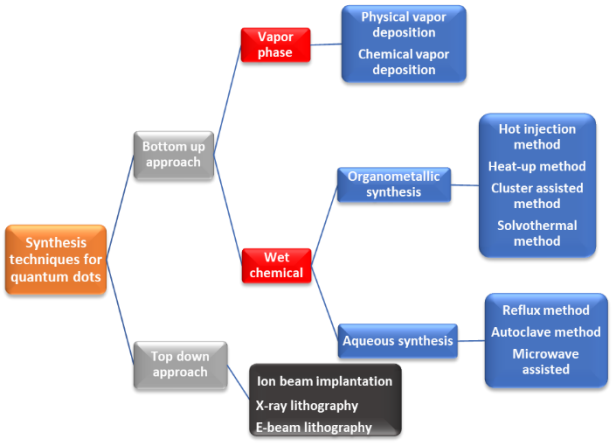

Figure 5: *Various Techniques for Synthesis of Nanomaterials.*

confinement effect including a considerable concentration of point defects in the lattice. Selecting a solvent is also an essential consideration for the wet chemical synthesis of QDs.[43] CdSe nanostructures using hot-injection method in aqueous solvent were synthesized successfully. CdSe particle sizes from 2.27 nm to 3.75 nm have controllable optical properties. The stabilizing agents such as TOP-TOPO, MPA, starch etc. used to synthesize high-quality CdSe QDs.[42] Generally, high-quality CdSe QDs occur in organic solvent through a hot injection method that employs long-chain hydrocarbon as ligands.[44]

Earlier, we recognized the efficient, one pot approach and easily scalable aqueous formation of starch capped CdSe QDs by photoirradiation and further explored its applications in detecting heavy metal ions.[8] CdSe QDs are among the most extensively studied and important II-VI semiconductors. It has optoelectronic properties due to very small size (in nm range) that is smaller than Bohr radius of exciton which is known as quantum confinement effect. QD are prepared using different methods as discussed above. The stable and highly luminescent QDs can be prepared using reactivity variation among Cd and Zn as well as Se and S precursors which have a wider range of emission wavelength (500-600nm)[45]. It focuses on the synthesis of CdSe QDs without requiring any extra additional reducing agent, no inert atmosphere or high temperature.[8] The TEM studies revealed that the size of QDs is very small which confirms the presence of strong confinement effect. QDs once extracted are used in the detection of Cu^{2+}, Hg^{2+}, and Cr^{6+} ions.[8]

Figure 5 summarizes the various methods for QD production, showing that top-down methods reduce bulk material sizes, while bottom-up methods use chemical precursors from group II-VI elements for QDs synthesis.

Top-down approach: It includes breaking down large pieces of particles into nanostructures. This approach is good for making structures with long-range order and macroscopic connections. Strategies utilized for top-down approaches are X-ray lithography and E-beam lithography.[47]

Bottom-up approach: It includes collecting single atoms into bigger nanostructures. This approach is best for gathering and building up short-range order at nanoscale measurements. Strategies utilized for bottom-up approaches incorporate pyrolysis, solvothermal forms, and sol-gel strategies.[47]

The synthesis method used can affect the size of the QDs, which in turn affects their characteristics and applications. This category can be divided into vapor phase and wet chemical methods.

Hydrothermal technique: A productive technique that creates QDs in an aqueous medium using an autoclave. Using this technique, inorganic salt is crystallized in an aqueous medium at a temperature and pressure that are regulated.[48]

The electrochemical method: An affordable technique that creates QDs with distinctive chemical and physical properties through electrochemical etching.[49]

Hot-injection: A novel method that produces homogeneous nucleation by supersaturating monomers through fast precursor injection. It is common practice to create monodisperse colloidal QDs using this technique.[50]

Microwave synthesis: A quick and affordable way to create QDs through microwave heating.

Ligand exchange: A well-studied method that uses bifunctional ligands to substitute the original ligands on the QD surface, making them water-soluble. This method is frequently employed for transferring QDs to an aqueous phase.

This category includes phase and wet chemical methods. Colloidal synthesis, a wet chemical method, has gained considerable interest in preparing QDs. Wet chemical methods are among the most widely used techniques for the synthesis of QDs. It includes the synthesis of QDs using aqueous and non-aqueous (organic) solvent. Various methods such as organometallic route, soft-chemical method, sonochemical method, hydrothermal method, electrochemical method are widely used methods for the formation of QDs. Another approach to preparing QDs is the photochemical process. Our group[21] had synthesized Cadmium selenide (CdSe) QDs in an aqueous solution, utilizing UV photo-irradiation with L-Cysteine as stabilizing agent.

As photochemical method does not require the use of hazardous chemicals and stringent laboratory conditions. The QDs prepared from this method were found to have tunable fluorescence.[23] CdSe QDs synthesized by wet chemical method is the most common route which involves organometallic precursor in a coordinating solvent.[24] A decrease in the diameter of the particles below approximately 10 nm leads to band gap enlargement and shifts toward the blue region and achieving the particle size about 3 nm in diameter.[24] Bansal *et al.*[29] have synthesized highly luminescent organic molecule capped Cadmium Sulphide (CdS) QDs with 69% PLQY in solutions.[29]

Ternary QDs have gained considerable interest in recent years. Mohanta *et al.*[30] reported bioconjugation of composite $Cd_{1-x}Zn_xS$-NCs (with x=¼ 0, 0.5 and 0.75). According to proponents of bioconjugate nanocrystals (NCs), the decay component resulting from free exciton recombination occurs nine times more quickly than the component resulting from surface recombination emission. By understanding the photoluminescence decay of bio-conjugated NCs contributes in the applications like biomolecular labelling, sensing and electrophysiology.[26]

Yakoubi *et al.*[31] reported low-cost aqueous synthesis of ternary QDs. They produced high quality CdZnS QDs, including those doped with Cu. They observed that the fluorescence and absorption spectra of CdZnS nanocrystals could be tuned by changing the stoichiometric ratio of Cd/Zn precursors in the host CdZnS QDs capped with different capping agents like 3-mercaptopropionic acid (MPA), L-cysteine, N-acetyl-L-cysteine (NAC), mercaptosuccinic acid (MSA), and glutathione (GSH). They successfully synthesized highly stable QDs and due to their favorable water dispersibility they can be used for biolabeling applications.[31] As the capping used was NAC, the photoluminescence quantum yield (PL QY) obtained was the highest (27%), MPA (9%) and GSH (3%).[31] The dots formed with NAC as a capping agent display the highest PL QY.[31]

One more work is reported where the synthesized QDs have impressive oxidation stability, acid stability, and photostability in both aqueous solutions and within the intracellular environment[32]. Zhan *et al.*[32] described a double-shell structure through one-pot aqueous synthesis via microwave assisted technique. The size obtained was very small (~3.2nm) which implies that the CdSe/CdS/CdZnS core-shell

QDs can serve as a favorable candidate for fluorescent QDs based biological applications due to its lower cytotoxicity.[33] Colloidal QDs may be applied in bulk solution or as a solid film.[39] The technique where the reactants typically interact in the gaseous phase at elevated temperatures and deposit on the surface of sample comes in the category of bottom-up approach method which is known as chemical vapor deposition.[46]

Table 1: *Synthesis of various QDs their particle size, band gap, and applications with references*

S.No.	QDs	Synthesis Route	Particle Size (nm)	Band Gap (eV)	Applications	References
1	ZnO	Green synthesis	5-10	3.37	Drug delivery	53
2	ZnS	Green synthesis	2-6	3.58	Used for fabrication	54
3	ZnSe	Wet chemical method	2-10	2.7	Vivo imaging and solar cells	55,56,57
4	CdO	Aqueous synthesis	2-3	1.36-2.3	In optoelectronic devices	58
5	CdS	Mechanochemical method	4-8	2.42	Economical approach for single-target-imaging application.	59
6	CdSe	Photochemical synthesis, electrochemical	2-7	1.91-2.84	Sensing heavy metal ions	7,20,21
7	CdTe	Aqueous synthesis	3.4	1.44	Making LEDs and sensors	4
8	CdZnS	Wet chemical method	<5	2.4-3.7	In optoelectronics devices (used as photo-conductive and heterojunction solar cells)	60,61
9	CdZnSe	Wet chemical method	2-4	1.5-3	Fabrication of QLEDs	62
10	$CuInS_2$	Solvothermal approach	2-4	1.5	Fabrication of affordable solar cells and enhanced efficiency	63

Aboulaich *et. al.*[31] reported synthesis of CdS via one-pot non-injection hydrothermal approach that involved cadmium chloride, mercaptopropionic acid (MPA, and thiourea as initial substances. The average size of QDs obtained is 3.5nm which has the highest photoluminescence i.e. 20%. The characterization of CdS@MPA QDs involved photoluminescence spectroscopy and UV-Vis, TEM, X-ray diffraction. As shown in figure 6(a) the UV−vis spectra of CdS@MPA QDs, synthesized with a Cd2+ /thiourea/MPA molar ratio of 1/1.7/2.3 and Cd2+ concentration of 5 mM, after different heating times (45 min, 1 h, 1.5 h, 2 and 3 h). The wavelength at which bulk CdS exhibits absorption edge is 515 nm. All samples, with the exception of CdS QDs that were heated for three hours, had distinct initial excitonic peaks at 363, 369, 382, 387, and 409 nm for 45 minutes, 1h, 1.5h, 2h, and 3 hours of heating, respectively. These peaks were linked to 1sh-1se excitonic transitions. The CdS sample's absorption spectra (t = 3 h) are wider, yet the variance of the absorption peaks shows that the particles expand quickly as the reaction time extends. The size dispersion gradually becomes less focused as a result of Ostwald ripening.[31] With time, PL intensity shifted towards red region. Fig 6 (c) shows digitally prepared QDs after 3h. It is shows PL emission between 375 and 460nm.The colloidal solution of the as prepared QDs after 3 hours is shown in fig. 6 (b).

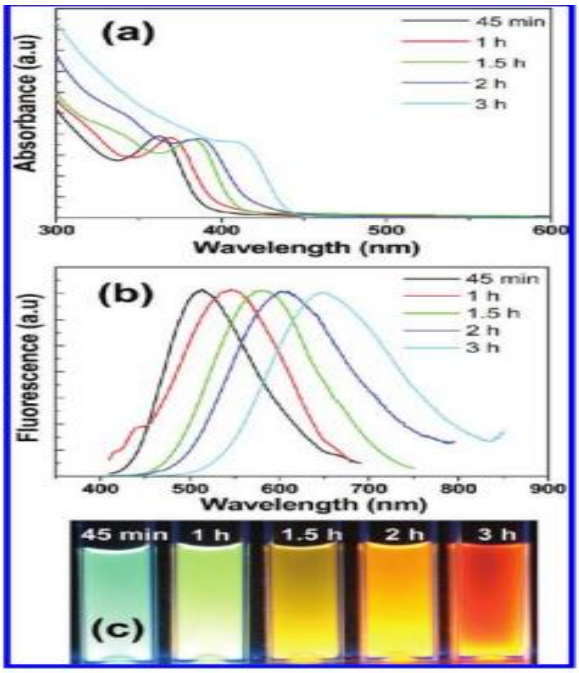

Figure 6 *(a) UV-Visible (b) PL Spectra of CdS@MPA QDs after different reaction times at 100° C (c) Digital picture of CdS under UV excitation (reproduced with permission from ref 19. copyright 2012).*

Other important characterization methods include transmission electron microscopy (TEM) and X-ray powder diffraction (XRD). Both provide the information about the crystal structure of the QDs. Furthermore, TEM also provides the exact shape and size of primary QDs. Broad peaks in the XRD pattern of CdS@MPA QDs indicate the sample's nano-

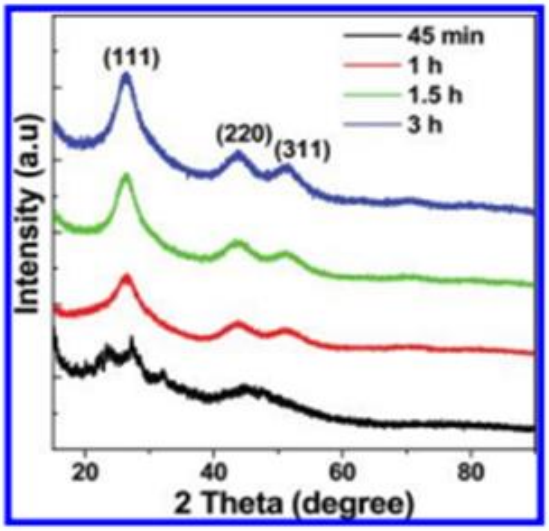

Figure 7: *XRD patterns of the as-prepared CdS@MPA QDs as a function of heating time (reproduced with the permission from ref 19. copyright 2012).*

scale size (Figure 7) The peaks are found at 2θ = 26.5°, 43.9°, and 51.6°, aligned with the (111), (220), and (311) directions, indicating that the nanoparticles have a cubic zinc blende form.[31]

Meng *et al.*[34] reported aqueous synthesis of ternary QDs i.e. CdZnS using solvothermal method.

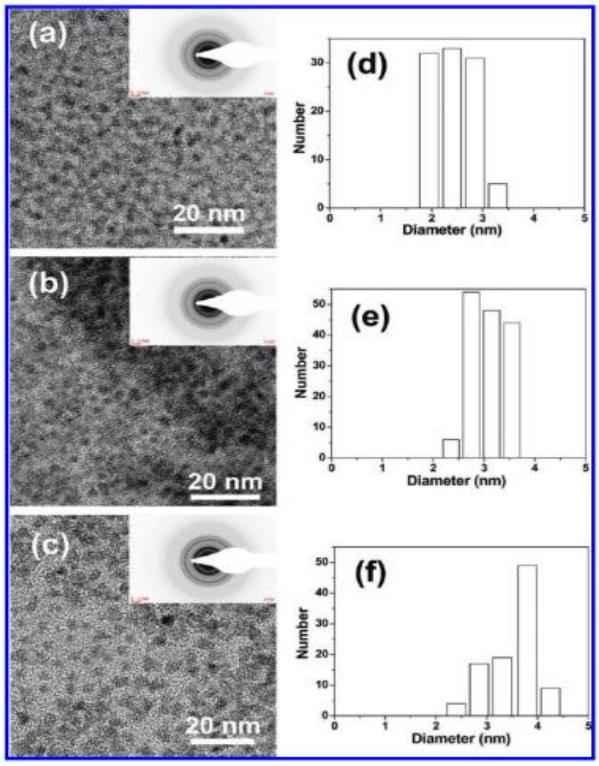

Figure 8: *TEM images of CdS nano crystallites prepared under hydrothermal conditions for (a) 45 min, (b) 1.5 h, and (c) 3 h. Insets show the SAED patterns. (d–f) Corresponding size distributions (reproduced with the permission from ref 19. Copyright 2012).*

Figure 8(a-c) display the TEM images of the CdS nanocrystallites that were prepared during 45 minutes, 1.5 hours, and 3 hours of heating, respectively. The corresponding selected area electron diffraction (SAED) patterns for CdS@MPA QDs are displayed in the insets of fig. 8 (a–c). The dependence of CdS QD particle size on heating duration is confirmed by figure 8 (d–f).

ZnCdS is a solid solution semi-conductor that combines the advantages of both ZnS and CdS materials by introducing ZnS into the lattice of CdS, resulting in a regulable crystal structure. The morphological and dimensional characteristics of the photocatalysts were investigated with scanning electron microscopy (SEM). As shown in figure 9 (a, b), the CdZnS QDs exhibit a uniform and regular surface morphology and the average size recorded was about 300 nm.

The XRD patterns of ZnCdS are illustrated in figure 10. The precursor pure ZnCdS exhibits prominent peaks at 2θ = 24.8°, 26.5°, 28.1°, 43.6°, 47.8°, and 51.8° aligning to (100), (002), (101), (110), (103), and (112) crystal planes of the hexagonal phase of CdS respectively.

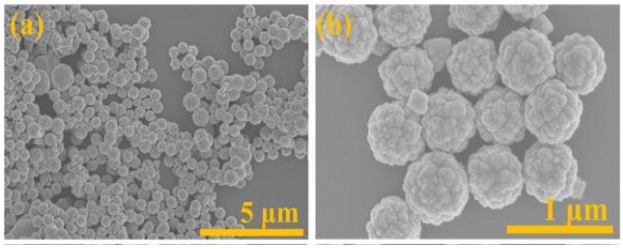

Figure 9: *SEM images of CdZnS QDs showing globular morphology (reproduced with the permission from ref 43. copyright 2024)*

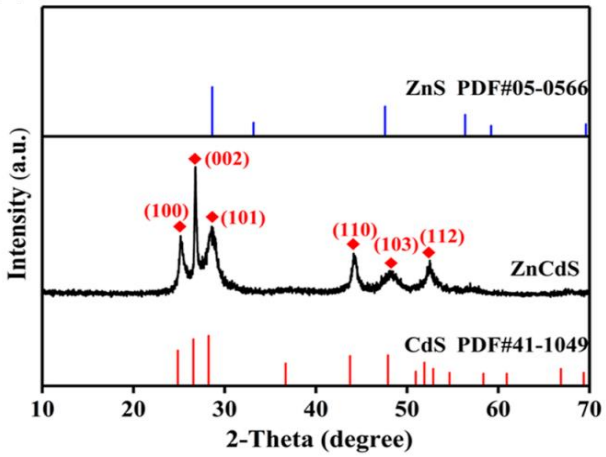

Figure 10: *XRD patterns of ZnCdS. and corresponding peaks of ZnS and CdS (reproduced with the permission from ref. 43. copyright 2024)*

3. Applications

Chalcogenide-based QDs have drawn prodigious research interest within optical-related devices, including photovoltaic cells, photodetectors, photosensors, photoelectrochemical devices, phototransistors, solar cells, catalysis, and drug delivery. When designing QDs for specific applications, several key factors should be considered, such as surface chemistry, size and shape, stability, toxicity, composition, and scalability. A variety of these applications are commercially accessible and have become integrated into our everyday lives (figure 11).

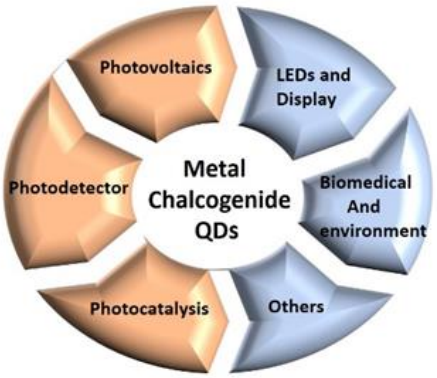

Fig. 11: *Applications of Chalcogenide-Based QDs*

Below we detail notable works based on these applications.

3.1 PHOTOVOLTAICS

Metal chalcogenide QDs have promising uses in photovoltaics, particularly in solar cell technology. Firstly, their tunable bandgaps enable the optimization of light absorption across various wavelengths, increasing, the efficiency of solar energy conversion. This tunability also allows for the production of multi-junction solar cells, in which layers of QDs can be tailored to absorb different sections of the solar spectrum. Absorber material, multiple sensitizations, intermediate-band solar cells, multiple exciton generation, and tandem solar cells are a few ways metal chalcogenide QDs can be utilized in photovoltaics.[65] Chen *et al.*[66] introduced devices used in photovoltaics that are equipped with nanomaterials to raise the energy conversion regulation and its efficiency. Devices made using chalcogenide QDs like CdS, CdSe, and CdTe in a liquid-type electrolyte have shown cell efficiencies lying from 3 to 6%.[67] This is significant because it demonstrates the potential of these materials help to design better-performing solar energy systems. Furthermore, various strategies are being explored to improve the photocatalytic water-splitting capability of metal chalcogenide QDs. These include cocatalyst, element doping, creating heterojunction, and plasmonic material photosensitization.[67] Alam *et al.*[69] reported the combination of CdSe QDs with ZnO nanowires to create hybrid solar cells with up to 50-60% internal quantum efficiencies and sensitized-type solar cells with an efficiency of power conversion of roughly 2.7%, which are based on TiO_2 inverse opal with CdSe QDs as sensitizers. Singh *et al.*[70] reported avenues for improvement used to modify the bandgap of QDs (CdSe and CdTe), such as post-synthesis chemical remedies, co-sensitization, deposition techniques, and doping of sensitizers.

Zhu *et al.*[71] introduced tandem solar cells that utilize lead chalcogenide (PbS, PbSe) QDs, which exhibit excellent quantum confinement effects and can include the full infrared range of solar radiation by changing their size. This makes them highly potential cost-effective infrared photovoltaic devices. The primary component influencing the CdS QDSSC performance, according to observations of Padmaperuma *et al.*[72], appears to be the ICR process at the CdS QD/TiO_2 interface. According to Mumin *et al.*[73] supercritical carbon dioxide synthesis was used to spread core-shell CdS/ZnS QDs into copolymers. Additionally, the layout of CdSe QD materials for converting energy purposes was helped by theoretical research using DFT calculations.[74] By simulating various surface modifications or doping scenarios using DFT calculations, researchers can explore strategies to enhance specific properties of metal chalcogenides QDs for applications such as solar cells, optoelectronic devices, sensors, and catalysis. A table summarizing the photovoltaic properties of various metal chalcogenide QDs is mentioned here.

Table 2: *Various Metal Chalcogenide-based QDs and Their Photovoltaic Efficiency*

QDs	J_{sc} (mA cm^{-2})	V_{oc} (V)	PCE (%)	Reference
CdS/CdSe	15.77	0.579	0.521	74
Zn-Cu-In-S	4.34	0.51	2.01	75
$CdSe_xTe_{1-x}$	20.78	0.653	8.21	76
$CdTe/CdSe_xT_{1-x}$	16.20	0.621	7.24	77
CdTe	2.10	0.68	0.87	78
Zn-Cu-In-Se	11.11	0.59	4.13	79
Zn-Cu-In-Se	26.49	0.77	13.85	80
$CuInS_2$	11.33	0.68	3.13	81
CdS/CdSe	32.247	0.629	8.28	82
Zn-Cu-In-Se	26.98	0.772	13.84	83
Zn-Cu-In-S-Se	25.51	0.78	14.4	84
CdSeTe	10.048	0.664	3.379	85

3.2 PHOTODETECTORS

QD photodetectors have applications in visible and IR-light cameras, machine vision, spectroscopy, and fluorescent biomedical imaging. Photodetection can be observed by different kinds of devices, like light-dependent resistors or photodiodes. The traditional photodetectors are bulk semiconductor based hence they are not very stable and flexible. In addition, they have expensive substrates, and the movement of charge carriers is restricted. QDs have been playing an important role in integrating these pre-existing technological platforms to enhance their performance[87]. Tang *et al.*[88] demonstrated a two-step ligand-exchange technique, by using this method an improved responsivity in PbS QDs photodetectors can be observed in the IR spectral region. Printing methods were also implemented to PbS QDs devices, including photodetector arrays[90], and broadband photoconductors.[89] IR photoconductive photodetectors are fabricated from Ag_2Se QDs.[91] By using a fast microwave-polyol approach, photoconductors were developed from highly packed PbS QDs films.[92]

Infrared photodetectors are broadly used in security monitoring, the vision of machines, autonomous automobiles, as well as other fields.[93,94] Traditional IR photodetectors are often based on materials like InGaAs and HgCdTe which offer commendable reliability, wide-band detection capabilities, high sensitivity, and long-time stability.[95] While effective, these materials suffer from limitations such as complex production processes, substantial fabrication costs, and poor compatibility with silicon-based readout integrated circuits.[96,97] Zhao *et al.*[98] have explored lead chalcogenide colloidal QDs (CQDs) (PbTe, PbSe, and PbS, etc.) to develop efficient and affordable IR photodetectors. Another exciting avenue is mercury chalcogenide CQDs, having similar advantages: solution processability, better compatibility with silicon substrates, and scant manufacturing costs. They hold great potential for use in IR imaging and detection.[99,100] CQDs show potential for dual-band photodetectors due to their changeable bandgaps. These photodetectors are garnering significant interest due to their promising applications in biological detection, environmental surveillance, and optical communication. They can process signals from both visible (VIS) and short-wave infrared (SWIR) wavebands, providing greater precision and detailed images of detected materials compared to single band detectors. Zhao *et al.*[101] have been exploring the detector utilizing HgTe along with CdTe CQDs as sensing layers. Between the layers of CdTe and HgTe, n-type ZnO is introduced. This layer achieves a responsivity of 0.5 AW^{-1} for the visible band (peaking at 700 nm) and 1.1 A W^{-1} for the SWIR band (peaking at 2100nm). The detectivity reaches 1.1 × 10^{11} Jones at +3V (for VIS) and 4.5 × 10^{11} Jones at -2V (for SWIR).

3.3 Photocatalysis

Metal chalcogenide QDs are useful in photocatalysis arising from their proficiency in absorbing light over an extensive range from UV to visible regions, hence increasing sunlight harvesting. Their nanoscale dimension allows for an extensive surface area and many active reaction sites. They

also allow to separate electron-hole pairs efficiently, lowering recombination and boosting charge carrier lifespan, which is critical for photocatalysis. Functionalization and hybridization with other materials can enhance their performance. Photocatalysts can be applied in a variety of processes, such as treatment of wastewater, conservation energy, self-cleaning applications, antifouling, sterilization, and air purification.[102,103] Some semiconductors can mineralize organic contaminants, such as halo hydrocarbons, aromatics, insecticides, pesticides, surfactants, and dyes. Mainly binary chalcogenides such as TiO_2, ZnO, CdS, ZnS, and Fe_2O_3 are utilized for photocatalytic properties. In addition to binary chalcogenides, some examples of ternary chalcogenides such as $SrZrO_3$, $PbCrO_4$, $CuInS_2$, Cu_2SnS_3, $XGaS_2$[104] (X= Ag or Cu), $SnSb_2S_5$ etc. and quaternary chalcogenides such as GeSbSeEr,[104] Cu_2ZnSnS_4 etc. have also been used. Exposure of photocatalysts to light of an appropriate wavelength causes an electron within the valence band to absorb photon energy and become excited in the conduction band, leading to the creation of a hole in the valence band simultaneously. These holes and electrons participate in redox reactions on the semiconductor's surface. A general reaction mechanism for the photocatalysis process can be represented as follows:

$$\text{Semiconductor} \xrightarrow{h\nu} \text{Semiconductor } (e^-(cb) + h^+(vb))$$

$$e^-(cb) + O_2 \longrightarrow O_2^{-\bullet}$$

$$h^+(vb) + H_2O \longrightarrow {}^{\bullet}OH + H^+$$

$$\text{Organic molecules} + {}^{\bullet}OH \longrightarrow \text{Degraded products}$$

The excited electron is capable of reducing substrates or combining with electron acceptors like O_2, whether present on the semiconductor surface or dissolved in water, thereby converting it to a superoxide radical anion $O_2^{-\bullet}$. The hole, in contrast, can oxidize organic molecules to produce R^+ or engage with ^-OH or H_2O to form $^{\bullet}OH$ radicals. Other highly oxidizing like peroxide radicals also contribute to the photodegradation of organic substrates. The $^{\cdot}OH$ radical is a very potent oxidizer and effectively decomposes azo dyes and pollutants. The photocatalysis process is explained in the figure given below (Figure 12):

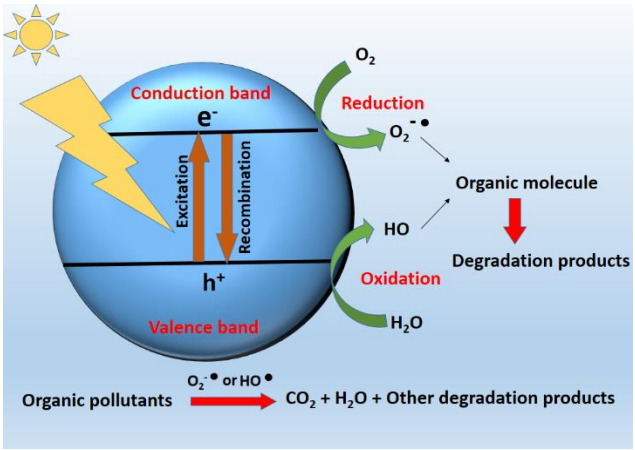

Figure 12: *Schematic of generation of exciton pair and their reaction in the photocatalysis process.*

Photocatalysts play a significant role in various applications, including pollutant degradation, hydrogen formation *via* water splitting, and carbon dioxide reduction. Metal chalcogenides contribute to accelerating photoreactions, driving advancements in these fields. Weiss and Weix *et al.* [106,107] demonstrated the Cd chalcogenide QDs were able to operate carbon-carbon coupling reactions. With the help of carbon QD-sensitized TiO_2/Pt nanocomposites, light-driven H_2 production was achieved.[108]

Enzymatic activation has been demonstrated separately by a ssembling DNA cells and CdSe/CdZnS/ZnS core shell and CdSe/ZnS core–shell QDs.[109] Metal chalcogenide QDs have been explored for photocatalytic air cleansing, including volatile organic compounds decomposition and the removal of air pollutants. Luminescent nanotags also be the application of metal chalcogenide QDs. Durmusoglu *et al.*[110] proposed using luminescent nanotags (hybrid coated PbS and PbS/CdS QDs) for authenticating fossil fuel products. Combining the luminescent properties of CdTe QDs with superparamagnetic maghemite (Fe_2O_3) cores, these QDs are hybrid nanoprobes. By incorporating these nanoprobes, one can efficiently detect and visualize defects or anomalies in materials submerged in water baths.[111] Meng *et al.*[112] created a catalyst for an effective photocatalytic nitrogen reduction process (PNMM) by loading bismuth metal on ZnCdS nanospheres. The photocatalyst´s ammonia generation efficiency was greatly enhanced by Bi nanoparticle under light. The 3% Bi@ZnCdS produced 58.93 $\mu molg^{-1}h^{-1}$ ammonia using lactic acid under air, nearly 7.7 times more efficient than pure ZnCdS.

3.4 LED and Display

One of the main applications of metal chalcogenide QDs is LEDs for the production of highly efficient and stable red, green, and blue light emissions. Metal chalcogenide QDs improve LEDs and display technologies by allowing for tunable emission qualities, which results in more brilliant colors and greater color purity. They enable more efficient light-emitting layers, which reduces energy usage and increases gadget lifespan. There are stability and lifetime concerns of organic LEDs and other LEDs. However, the QDs-based LEDs are inherently stable and have a longer lifetime. The lifetime of LEDs is affected by various factors like- oxidation, heat, exposure to UV light, etc. Various strategies like- cre-shell engineering, surface passivation, and architecture optimization are adopted to improve the lifetime of QDs.These QDs can often be carefully designed to emit light at specific wavelengths, which makes them useful for developing a variety of colors for LED displays and lighting applications. Furthermore, metal chalcogenide QDs have also been used to enhance the color rendering index (CRI) of LEDs, leading to more accurate and natural color reproduction. Additionally, metal chalcogenide QDs can be used to enhance the stability and lifetime of LEDs by improving their resistance to environmental influences including humidity and temperature. The PbX QDs can effectively be utilized in NIR-QLEDs with the ability to tune their emission wavelength by altering the size of QDs. The first PbX-based NIR-QLEDs achieved an external quantum efficiency (EQE) of 0.5%. Notably, EQE of NIR-QLEDs has enhanced from 2% in 2012 to 7.9% in 2018.[113-117] The equation[115] below can be utilized to calculate the efficiency of EQE of NIR-QLEDs**:**

$$EQE = \eta_{diff} * \eta_{inj} * \eta_{PLQY} * \chi * \eta_{out}$$

Where, η_{diff} - efficiency of injected carriers that successfully diffuse to QDs.

η_{inj} - efficiency of these carriers that transfer into QDs and form excitons.

χ - efficiency of these excitons whose states have spin-allowed optical transitions (for colloidal QDs, χ =1).

η_{PLQY} - internal QD PL QY, &η_{out} = light out-coupling efficiency.

η_{diff} and η_{inj} are two key parameters for the efficiency of NIR-QLED devices. In visible-QLEDs, it is important to choose suitable carrier transport layer materials[118,119] to enhance η_{inj}.

The use of Cd-based QDs aims to augment material properties in conjugation with the developed shell and surface ligand.[120,121] According to Pal *et al.*[122], the performance of the device is affected by the thickness of the CdSe shell that encases the CdSe core of the QDs. Consequently, they achieved a maximum EQE with a 13-layer of the CdS shell, resulting in a brightness of about 1000 cdm^{-2} at a low starting voltage of approximately 3V.

Chen *et al.*[123] introduced a technique to develop a shell layer that reduces blinking in QDs by disregarding the lattice discrepancy within the core and shell. Cadmium (II) oleate and octanethiol are employed as precursors to create high-quality CdSe/CdS core/shell QDs, effectively minimizing lattice mismatch. The PL peak width dropped from 96.2 meV for uncoated CdSe QDs to 67.1 meV for final results CdSe/CdS QDs (20nm), the highest PL QYs of 97% was observed, and 94% average on-time fractions, indicating significant suppression of blinking.

Pu *et al.*[124] presented the concept of an electrochemically stable surface-binding ligand. T_{50} > 3800 hours at 1000 cdm^{-2} for red-emitting LEDs and T_{50}> 10,000 hours at 100 cdm^{-2} for blue-emitting LEDs were achieved using the electrochemical inert ligand. Kim *et al.*[125] reported blue QDs created from layers of ZnS, ZnTeSe, and ZnS QDs for the advancement of InP-based QDs. They attained a full width at half maximum (FWHM) of 23 nm, with PL QYs of 85%. The EQE was 6.8% at 3.6 V and exhibited a peak luminance of 14146 cdm^{-2} was achieved. Jiang *et al.*[125] proposed a In^{3+}-doped strategy in Zn-Cu-Ga-S@ZnS QDs. Resulting PLQY value 95.3% was achieved. In ZnCuGaS:In@ZnS, maximum luminance 1402 cdm^{-2} and EQE 2.4 % was also achieved which gave a high CRI value of 94.9. Based on this red, green, and blue photoluminescence/electroluminescence (PL/EL) spectrum of a single-component QD that is stable and balanced, meeting the requirement of lighting and display.

Hexagonal boron nitride sheets are incorporated in order to strengthen the thermal stability of devices constructed from CdSe/CdS QDs[127]. Additionally, $CuInS_2$/ZnS QDs with dependable thiol-based ligands and amino-based ligands are recommended for the efficient development of film-type display devices[128].

Table 3: *A summary of metal chalcogenide-based LED and display materials.*

QD Materials	Method	Performance Summary	Reference
CdSe	Maximization of shell thickness efficiency	Achieving 1000 cdm^{-2} luminance with a 3 V turn-on voltage.	88
CdSe	Shell layering kinetics control for suppression of lattice mismatch	PL QYs 97%, FWHM 67.1 meV (20 nm).	89
CdSe	Electrochemically stable ligands	T_{95}> 3800 h at 1000 cd m^{-2} luminance for red emission T_{50} surpasses 10,000 h at 100 cd m^{-2} for blue.	90
ZnTeSe	ZnS/ZnTeSe/ZnS quantum well structure	EQE 6.8% at 3.6V, luminance 14146 cd m^{-2}, FWHM 23 nm.	91
ZnCuGaS:In @ZnS	Ln^{3+}-doping	PLQYs 95.3%, EQE 2.4%, luminance 1402 cdm^{-2}	92

3.5 Biomedical

Metal chalcogenide QDs help to promote biomedical imaging by providing improved luminescence, which improves picture quality and sensitivity. Their size-dependent optical features enable tunable emission wavelengths, allowing for multi-color imaging and tracking of many targets at the same time. Researchers are involved in the reduction of the toxicity of chalcogenide QDs for their use in biological applications by their surface functionalizing with biocompatible coatings, investigating less toxic core compositions, controlling QD size and dosage, and utilizing bioconjugation for targeted delivery. Their surface alterations allow for focused imaging of certain cells or tissues, which improves diagnostic accuracy. Furthermore, metal chalcogenide QDs have extended photoluminescence lifetimes and are resistant to photobleaching, increasing the reliability and duration of imaging experiments. Overall, these characteristics make them useful instruments for cancer diagnosis and immediate tracking of biological processes. In the biomedical field, the numerous uses of metal chalcogenide QDs such as bioimaging, single-QD tracking of extracellular and intracellular targets, therapeutics, fluorescence resonance energy transfer (FRET), gene technology, detection, etc.[129] Their small size, high quantum yield, and tunable emission wavelengths make them ideal for labeling and tracking biological molecules and cells in living systems. They can be constructed to focus on certain tissues or cells, making them useful for therapeutic delivery and intervention. QDs have been employed for different applications both in vivo and in vitro imaging. In 1998, the research teams of Alivisatos and Nie separately presented the first examples of a QD system in bioimaging. Su *et al.*[130] developed a sensor to measure pH inside the cells utilizing $AgInS_2$/ZnS QDs to differentiate between cancerous and healthy cells. This pH sensor can be used to image living cells with in various pH solutions and and cell lines by combining QDs with fluorescent lifetime imaging microscopy. Interestingly, this sensor examined the cervical cells that were ejected from 20 patients. According to findings, this sensor can provide a higher sensitivity to traditional cytology in the clinic, opening the door for effective noninvasive cervical cancer screening. In the context of COVID-19, metal chalcogenide QDs have been explored for their potential in bioimaging, biosensing, and even in therapies targeting virus.[131] They can be engineered for prompt theranostic applications of severe acute respiratory syndrome coronavirus 2 (SARS-CoV-2). Several II-IV QDs are known as fluorescent markers for bioimaging applications. For example, the CdSe/ZnS QDs linked with streptavidin and immunoglobulin G (IgG) are used to image the breast cancer cells through the recognition of HER2 biomaker[132] while $CuInS_2$/ZnS QDs, which have low nonspecific binding and easily conjugated to other molecules, making them useful cell imaging markers.[133] Additionally, Nguyen *et al.*[134] demonstrated $CuInS_2$/ZnS (CIS/ZnS) QDs that were linked to neutravidin served to trace biotinylated actin. Bioconjugated QDs are highly useful in targeted drug delivery, gene delivery, bioimaging, pathogen detection, etc. Li *et al.*[135] synthesized biocompatible Mn-doped $CuInSe_2$ QDs functionalized with folic acid that had a fluorescence performance of 31.2% in NIR-II. These QDs are found to gather mostly in 4T1 breast cancer tumors and can be utilized for NIR fluorescence imaging. Clinical diagnostics CA125, a very sensitive test for an ovarian tumor marker, was introduced with the help of CdTe QDs and SiO_2@polydopamine core-shell nanoparticles.[136] Freitas *et al.*[137] demonstrated that CdSe/ZnS QDs were used to identify HER-2-ECD breast cancer cells´ biomarkers (CA15-3) while CdSe/ZnS QDs associated with antibodies to trace the presence of breast cancer cells.[138] Protein measurements, protein interaction monitoring, and enzyme activity assays have all taken advantage of the conformational shift resulting from FRET. Forester resonance energy-transfer method was used to modify CdSe/CdS/ZnS QDs and antibodies markered with terbium to create a sensor that can detect adenosine diphosphate.[139] In bacterial cells and model membranes, CdSe and ZnSe together with a ZnS Shell appeared membrane disturbance activity.[140] CuInS/ZnS QDs with infrared emission were developed by Lv *et al.*[141] for tumor phototherapy. These QDs effectively obtained bimodal tumor treatment using PDT and PTT. Under 660 nm laser irradiation, the tumor cells were successfully eradicated from

the mice by the combined actions of photothermal and photodynamic effects.

3.6 Environmental Applications

In environmental applications, metal chalcogenide QDs have been explored for use in environmental sensing and monitoring. Their high sensitivity and selectivity and fast response time make them useful for detecting and monitoring various environmental pollutants which consist of organic pollutants, heavy metals, as well as microbes. They may additionally be used for environmental remediation, such as removing pollutants from water or soil. Blue fluorescent WS_2 QDs have exhibited high sensitivity (K_D = 1.1× 10^4 M^{-1}) and selectivity for ferric ions[142] (Fe^{3+}) while for 2,4,6-trinitrophenol, melamine, and Cu^{2+}, surface-functionalized $MoSe_2$ QDs worked as chemosensors.[143] It has been demonstrated by our group that starch-capped CdSe QDs functionalized with thiourea were used to sense heavy metal ions in aqueous solutions[8]. The metal ions Cu^{2+}, Hg^{2+}, and Cr^{6+} particularly quenched the PL intensity of CdSe QDs. Resulting, Cu^{2+} ions show lower limit of detection (LOD) (27.6 µM) than both Hg^{2+} (196 µM) and Cr^{6+} (279.2 µM) ions. Wei *et al.*[144] demonstrated that QDs could detect the Cd^{2+} ions by increasing the fluorescence intensity through aggregation-induced emission, using Zn-Ag-In-S (ZAIS) QDs capped with L- cysteine. CdSe gel gas sensors fabricated using an electrogelation method have shown exceptional performance for NO_2 gas sensing at room temperature, which is crucial for air quality monitoring.[145]

Using metal chalcogenide QDs in a variety of applications can have serious environmental consequences. Toxic metals such as cadmium and lead may be released during manufacture and disposal, posing dangers to soil and water systems. Furthermore, the synthesis methods frequently produce toxic byproducts. Proper waste management and the development of less harmful alternatives are critical for mitigating these environmental concerns.

Toxic gases can be harmful to ecosystems and human health, making their presence in the environment a major global problem. Anthropogenic sources such as power plants, manufactures, or smoke are the major source for hazardous gases (such as NH_3, CO_x, H_2S, SO_x, and NO_x that have been released into the atmosphere. Human senses are unable to identify several of the hazardous gases at low amounts, and some of the gases have no smell at all.[146] Geng *et al.*[147] developed a feasible approach for detecting NO_2 gas at room temperature employing a PbSe QD gel substrate. Firstly, CdSe QD gels were created and then converted into PbSe QD gels via a cation exchange method. The gas sensing was conducted under various LED light irradiation conditions, with the greatest findings achieved under violet light illumination. The sensor responded linearly to NO_2 concentrations ranging from 0.003 to 1.32 ppm, with a low LOD of 3 ppb and excellent response/recovery times (27 and 102 s). The scientists employed heavy metal QDs to create a NO_2 sensor with a lower LOD at room temperature. Under UV irradiation at 40 °C, the ZnO/SnO_2 composite (SZQ1%) with a molar ratio of 1:100 demonstrates outstanding NO_2 gas detecting characteristics with a LOD of 100 ppb.[148] Lin *et al.*[149] created a flexible and portable NO_2 sensor by modifying nylon fibres with ZnO QDs and reducing graphene oxide (rGO. The sensor has a linear response from 20 to 100 ppm and a LOD of 20 ppm at 25°C. The sensor performed well with response and recovery times of about 216 seconds and 668 seconds, respectively. The scientists incorporated the portable fibre sensor with an electrical module to create an over-limit monitoring system for NO_2 values above 20 ppm. Liu *et al.*[150] created $CuSbS_2$ QDs/rGO composites *via* hot injection to make gas sensors. The composites showed high NH_3 detection ability at room temperature (23 ^oC) and a low LOD of 500 ppb. Furthermore, the sensor demonstrated excellent selectivity and rapid response/recovery times of 50/115 s. To detect NH_3 gas, Sharma *et al.*[151] developed two-dimensional (2D) tungsten disulpide (WS_2) nanosheets coated by tin oxide (SnO_2) QDs. Low NH_3 concentrations resulted in a low LOD (~10 ppb) and high sensitivity (~175% ppm^{-1}) due to the improved response. When analyzed to WS_2 QD as CO_2 gas sensor, the Ru@WS_2 QD exhibits fewer impacts under various humid circumstances.[152]

3.7 Quantum Computing

Quantum computing has a wide area of uses and has numerous future benefits including drug design & development, computational chemistry, cleaner fertilization, electronic materials discovery, solar capture, better batteries, cybersecurity & cryptography, financial modeling, artificial intelligence& machine learning. QDs are a possible method for quantum computing that has gained traction as potential building blocks for solid-state quantum devices in recent years. QDs provide a platform for investigating several ways of approaching quantum computation, such as information storage, quantum gate operations, and qubit implementation. QD technology is demonstrating potential in solid-state quantum computation and offers avenues for implementation in quantum information processing (figure 13).[153]

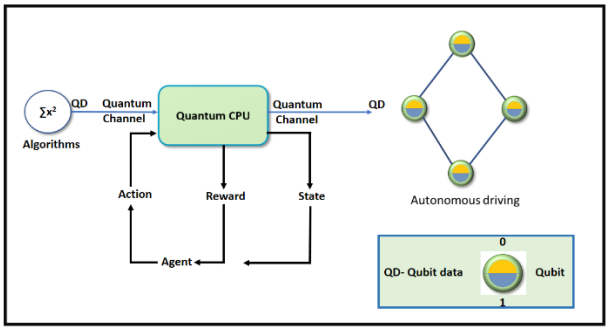

Fig. 13: *Flow chart illustrating the role of QDs in quantum computing.*

To further the capabilities of quantum computing, researchers are currently actively investigating and creating QD-based technologies. Nonetheless, there are a few obstacles to be addressed, like qubit interactions and manufacturing flaws, which restrict the use of QDs in the realm of quantum computing. The key to overcoming qubit interactions is regulated interactions between adjacent qubits. Even with these great advancements, there is still much work to be done to produce reliable and strong qubit interactions. Errors and noise can enter the system as a result of fabrication flaws, which can result in misleading calculations. Therefore, to simplify the scaling-up of QDs in the realm of quantum technologies, a precise controlled synthesis methodology is essential. Systems encoded within QDs have fewer internal degrees of freedom and are more effectively isolated from the outside world than systems with higher dimensions. There is growing interest in the possible uses of QDs for solid-state quantum computing because of these two properties, which are help extend the coherence periods of the qubit states contained within the dot.[154]

3.8 Neuromorphic/Memory

QDs have a wide band gap and high electron mobility. This enables them beneficial for advanced electronic devices like floating gate memory systems and neuromorphic hardware devices. Semiconductor QDs are a popular choice for photonic applications due to their compatibility with (Complementary Metal-Oxide-Semiconductor) CMOS-based processing methods. These devices offer great optical absorption, structural stability, and cost-effective production for vast area coverage. The density of states, band gap, material properties also surface effects (nature of the capping agent) govern the electronic properties of QDs that are very

significant for photonic applications and affect their performance in electronic devices. A rapid way to recover the performance was achieved by Jeong *et al.*[155] of CdSe QD floating gates utilizing low-intensity light. The concept of using QDs as the active element in memristors has become more and more favored in recent times due to its advantages, which include high quality, the ability to integrate with electronic devices, and low power consumption. Wu *et al.*[156] determined a ZnO/$CsPbBr_3$ QDs-based memristor with a low operating voltage (1V) and a high ON/OFF ratio (>105). Spintronics also has garnered a great deal of interest recently as a potential field for next-generation electronics due to its ability to reduce energy consumption and increase performance in classic electronics. It is utilizing the electron's spin state in QDs to create new electrical devices. Researchers are investigating metal chalcogenides due to their potential for energy-efficient neuromorphic computing. Neuromorphic computing aims to mimic the brain's computational abilities, emphasizing low power consumption and parallel processing. In terms of energy consumption, the human brain is about 10^6 times more efficient than typical CMOS logic. Low–range stimuli can trigger short-range mechanisms like structural phase shifts and coupled electron systems. These materials have the potential to create effective synaptic devices and memristors in neuromorphic systems.[157] Neuromorphic memristors derived from 2D TMCs hold great potential in brain-inspired computing and high-performance AI.[158] Using 2D materials in vertical memristors allows for scaling to thicknesses of 10 nm or even less, resulting in reduced operating voltage and great integration density. This is advantageous for less power applications[159]. Xu *et al.*[160] discussed advancements in neuromorphic optical and electronic devices, aiming to imitate the human brain to improve efficient energy use and data processing performance. Brain-like chips and in-memory computing systems benefit from PCM-based devices. The all-around benefits of QDs for memory applications include regulated sizes with flexible changes, emission properties, high optical stability, and tunable absorption. These benefits allow the memory architecture to have desirable features like uniformity, scalability, photoswitching, and flexibility.[161]

4. Challenges & Future's Perspective

Metal chalcogenides have various applications due to their interesting properties. However, they also face several challenges in different fields. Many metal chalcogenides, particularly those containing selenium and tellurium, can become unstable when exposed to light, heat, and moisture over a sustained period, resulting in decreased performance. QD surface imperfections can trap charge carriers, resulting in non-emissive recombination. These defects can affect the efficiency of QDs in photovoltaics and LEDs.Some chalcogenides, including those containing cadmium (e.g., CdTe), are hazardous, raising environmental and health problems. Cadmium-based QDs can induce apoptosis, altered gene expression, neurotoxicity, and mitochondrial damage. This hinders their applicability in biological and clinical imaging. To overcome this problem, scientists are investigating alternate materials and formation processes to create non-toxic QDs with preferred qualities. Inefficient Na^+ diffusion in chalcogenides can affect battery performance and Low electrical conductivity reduces rate capabilities. Ensuring the biocompatibility of QDs in biomedical applications is a significant challenge. QDs can release harmful ions in a biological environment, which is a major problem. Metal chalcogenide QDs are difficult to synthesize and require specialized equipment, limiting their applicability in many applications. Large-scale production of QDs involves issues such as maintaining consistent size and shape, efficiently scaling up synthesis methods, assuring purity and stability, and controlling environmental and safety concerns related to toxicity.

The major ongoing research on the chalcogenide QDs is in the biomedical application which aims to explore a greener and more scalable technique for the formation of these QDs. The future perspective of research and development also aims to replace the heavy and toxic metal ions with biocompatible metals like Zn, and Cu. The other challenge is to have precise control over shape, sizes and sizes, hence enhanced quantum yield and the other properties of these QDs. Overall, the future of research and development of chalcogenide QDs looks very promising and bright. The prospect of the use of QDs lies in the extensive work in the field of quantum computing, single photon emitters, and in spintronics, artificial intelligence. Integration of chalcogenide QDs with the perovskite QDs is also very interesting and challenging for improved photovoltaic performance.

5. Conclusion

Recent advances in chalcogenide QDs for practical applications consist of the creation of cadmium-free QDs, non-toxic, like those based on indium phosphide, which improve their environmental and health safety. Improved synthesis processes have allowed for greater control over size and shape, resulting in more consistent and efficient performance. Surface passivation processes have also been developed to improve stability and reduce deterioration. These improvements have increased the utilization of QDs in applications such as display technology, solar cells, and bioimaging, making them more commercially viable. In conclusion, Metal chalcogenide QDs offer a promising platform for various applications due to their distinctive physical and chemical features. The creation of metal chalcogenide QDs has advanced significantly over the years. Various approaches have been developed to achieve detailed control over the size, shape, and composition of these nanomaterials. Further, it is vital to improve the synthesis methods by exploring new precursors, solvents, and reaction conditions. This will allow for better control over QDs size distribution and surface passivation. These QDs have been widely studied for their potential applications in optoelectronic devices, solar cells, photocatalysis, and bioimaging due to their attractive properties that is high energy emission, and excellent photostability, and high quantum yield. The use of QDs in a variety of sectors has produced encouraging outcomes and created new opportunities for research and development. However, challenges including reproducibility, toxicity and stability require to be tackled for practical applications of metal chalcogenide QDs. Efforts are being made to develop eco-friendly synthesis techniques and surface modification ways to improve their biocompatibility and stability. Further investigation is required to explore the capability of metal chalcogenide QDs in emerging fields such as quantum computing and biomedical applications. Overall QDs are a fascinating area of research. Continued study and development in this area will certainly lead to exciting new advances in various technological fields.

Author Contribution Declaration

Pratibha and Aayushi conducted the literature survey together. Pratibha focused on writing the application section, while Aayushi worked on the introduction and synthesis sections. Both collaborated with Avinash to design the images. Avinash prepared the manuscript draft and contributed to the writing of the discussion and conclusion.

Data Availability Declaration

There are no new data were created hence data sharing is not applicable here.

Acknowledgements

The authors acknowledge the administration of SRM University Delhi-NCR, Sonepat for their support and encouragement.

References

1. J. Mal, Y. V. Nancharaiaha, E. D. van Hullebusch, P. N. L. Lens. Metal Chalcogenide quantum dots: biotechnological synthesis and applications. *RSC Adv*. **2016**, 6, 41477. https://doi.org/10.1039/c6ra08447h
2. L. Manna. The Bright and Enlightening Science of Quantum Dots. *Nano Lett.* **2023**, *23,* 9673. https://doi.org/10.1021/acs.nanolett.3c03904
3. C. B. Murray, D. J. Norris, M. G. Bawendi. Synthesis and characterization of nearly monodisperse CdE (E= S, Se, Te) semiconductor nanocrystallites. *J. Am. Chem. Soc.* **1993**, *115,*8706. https://doi.org/10.1021/ja00072a025
4. M. Gusain, R. Nagpal, Y. Zhan. Analysis and characterization of quantum dots. *Graphene, Nanotubes and Quantum Dots-Based Nanotechnology*, **2022** ch 29, pp 709-726. https://doi.org/10.1016/B978-0-323-85457-3.00027-X
5. K. T. Yong; W. C. Law, I. Roy, Z. Jing, H. Huang, M. T. Swihart, P. N. Prasad. Aqueous phase synthesis of CdTe quantum dots for biophotonics. *J. Biophotonics* **2011**, *4*, 9. https://doi.org/10.1002/jbio.201000080
6. R. K. Kesrevani, A. K. Sharma. Nanoarchitectured Biomaterials: Present Status and Future Prospects in Drug Delivery. *Nanoarchitectonics for Smart Delivery and Drug Targeting* **2016**, ch 2, pp 35-66. https://doi.org/10.1016/B978-0-323-47347-7.00002-1
7. N. Thejo Kalyani, S. J. Dhoble. Introduction to nano materials. Editor(s): N. Thejo Kalyani, Sanjay J. Dhoble, Marta Michalska-Domańska, B. Vengadaesvaran, H. Nagabhushana, Abdul Kariem Arof, *In Woodhead Publishing Series in Electronic and Optical Materials, Quantum Dots, Woodhead Publishing* **2023**, pp 3-40. DOI: https://doi.org/10.1016/B978-0-323-85278-4.00010-6
8. A. Singh, A. Guleria, S. Neogy, M. C. Rath. UV induced synthesis of starch capped CdSe quantum dots: Functionalization with thiourea and application in sensing heavy metals ions in aqueous solution. *Arab. J. Chem*. **2020**, *13*, 3149. https://doi.org/10.1016/j.arabjc.2018.09.006
9. T. Arfin, V. K. Alam, P. G. Moradeeya. Metal oxide photonic crystals and their application (designing, properties, and applications), (Ed.), S. Sagadevan, J. Podder, F. Mohammad, In Metal Oxides, Metal Oxides for Optoelectronics and Optics-Based Medical Applications, *Elsevier*, **2022**, pp. 191-204, https://doi.org/10.1016/B978-0-323-85824-3.00010-5
10. M. Bouroushian. Chalcogens and Metal Chalcogenides. *Electrochemistry of Metal Chalcogenides*, **2010**, ch 1, pp-1-56. https://doi.org/10.1007/978-3-642-03967-6
11. O. I. Micic, A. J. Nozik. Synthesis and characterization of binary and ternary III-V quantum dots. *J. Lumi*. **1996**, *70,* 95. https://doi.org/10.1016/0022-2313(96)00047-6
12. N. Chand, S. C. Thakur, P. B. Katyal, V. Barman, P. Sharma. Recent developments on the synthesis, structural and optical properties of chalcogenide quantum dots. *Sol. Energ. Mat. Sol. C*. **2017**, *168,* 183. http://dx.doi.org/10.1016/j.solmat.2017.04.033
13. L. Jing, S. V. Kershaw, Y. Li, X. Huang, Y. Li, Andrey L. Rogach, M. Gao. Aqueous Based Semiconductor Nanocrystals. *Chem. Rev.* **2016**, *116*, 10623. https://doi.org/10.1021/acs.chemrev.6b00041
14. A. Kiczor, P. Mergo. Synthesis of CdSe Quantum Dots in Two Solvents of Different Boiling Points for Polymer Optical Fiber Technology. *Materials* **2024**, *17*, 227. https://doi.org/10.3390/ma17010227
15. T. Arfin. Emerging trends in lab-on-achip for biosensing applications, In: C. M. Hussain, S. K. Shukla, G.M. Joshi (Eds.), Functionalized nanomaterials based devices for environmental applications: a volume in micro and nano technologies, *Elsevier, Netherland*, **2021**, pp. 199-218. https://doi.org/10.1016/B978-0-12-822245-4.00008-8
16. H. Huang, W. Feng, Y. Chen, J. Shi. Inorganic nanoparticles in clinical trials and translations. *Nanotoday* **2020**, *35*, 1. https://doi.org/10.1016/j.nantod.2020.100972
17. O. A. Aladesuyi, O. S. Oluwafemi. Synthesis strategies and application of ternary quantum dots - in cancer therapy. *Nano-Struct. Nano-Obj.* **2020**, *24*, 100568. https://doi.org/10.1016/j.nanoso.2020.100568
18. F. Mohammad, T. Arfin, H. A. Al-Lohedan. Development of graphene-based nanocomposites as potential materials for supercapacitors and electrochemicals cells, In: M. Jawaid, A. Ahmad, D. Lokhat (Eds.), Graphene-based nanotechnologies for energy and environmental applications: *Micro and nano technologies,* 1st Edition, Elsevier, Netherland, **2019**, 145-154. https://doi.org/10.1016/B978-0-12-815811-1.00008-9
19. D. Bera, L. Qian, T. K. Tseng, P. H. Holloway. Quantum Dots and Their Multimodal Applications: A Review. *Materials (Basel)* **2010**, *3*, 2260. https://doi.org/10.3390/ma3042260
20. K. Surana, P. Singh, H. Rhee, B. Bhattacharya. Synthesis, characterization and application of CdSe quantum dots. *J. Ind. Eng. Chem.* **2014**, *20*, 4188. https://doi.org/10.1016/j.jiec.2014.01.019
21. A. Singh, A. Kunwar, M. C. Rath. L-Cysteine Capped CdSe Quantum Dots Synthesized by Photochemical Route. *J. Nanosci. Nanotechnol*. **2017**, *17*, 1. DOI:http://dx.doi.org/10.1166/jnn.2018.14687
22. M. Saad, S. Nadi, F. Ibraheem, Y. A. Badr, I. A. Mahdy, Z. M. A. El-Fattah, A. Sayed. Bright photoluminescence from CdSe quantum dots conjugated with metal phthalocyanines. *Optical Mater.* **2024**, *147*, 114736. https://doi.org/10.1016/j.optmat.2023.114736
23. J. Drbohlavova, V. Adam, R. Kizek, J. Hubalek. Quantum Dots-Characterization, Preparation and Usage in Biological Systems. *Int. J. Mol. Sci.* ***2009***, *10*, 656. https://doi.org/10.3390/ijms10020656
24. K. Agarwal, H. Rai, S. Mondal. Quantum dots: an overview of synthesis, properties, and applications. *Mater. Res. Express* **2013,** *10*, 062001. https://doi.org/10.1088/2053-1591/acda17
25. T. Arfin, P. Ranjan, S. Bansod, R. Singh, S. Ahmead, K. Neeti. Organic electrodes: An Introduction, In: R.K. Gupta (Ed.), Organic electrodes: Fundamental to advanced emerging applications, Springer, Switzerland, **2022**, pp. 1-26. https://doi.org/10.1007/978-3-030-98021-4_1
26. B. Gao, C. Shen, S. Yuan, Y. Yang, G. Chen. Synthesis of Highly Emissive CdSe Quantum Dots by Aqueous Precipitation Method. *J. Nanomater*. **2013**, *19,* 1. http://dx.doi.org/10.1155/2013/138526
27. R. Lia, L. Tang, Q. Zhao, K. S. Teng, S. P. Laue. Facile synthesis of ZnS quantum dots at room temperature for ultra-violet Photodetector applications. *J. Chem. Let.* **2017**, *742,* 137127. https://doi.org/10.1016/j.cplett.2020.137127
28. S. Bansod, T. Arfin, R. Singh, S. Ahmad, K. Neeti. Chemically modified carbon nanotubes for lab on chip devices, In: J. Aslam, CM. Hussain, R. Aslam (Eds.), Chemically modified carbon nanotubes for commercial applications, Wiley-VCH GmbH, Germany, **2023**, pp. 271-298. https://doi.org/10.1002/9783527838790.ch12
29. A. Valizadeh, H. Mikaeili, M. Samiei, S. Farkhani, N. Zarghami, M. kouhi, A. Akbarzadeh, S. Davaran. Quantum dots: synthesis, bioapplications, and toxicity. *Nanoscale Res. Lett*. **2012**, *7,* 480. https://doi.org/10.1186/1556-276X-7-480
30. K. J. Nordell, E. M. Boatman G. C. Lisensky. A Safer, Easier, Faster Synthesis for CdSe Quantum Dot Nanocrystals. *J. Chem. Educ.* **2005**, *82*, 1697. https://doi.org/10.1021/ed082p1697
31. A. Aboulaich, D. Billaud, M. Abyan, L. Balan, J. J Gaumet, Ghouti Medjadhi, J. Ghanbaja, R. Schneider. One-Pot Noninjection Route to CdS Quantum Dots via

Hydrothermal Synthesis. *ACS Appl. Mater. Interfaces* **2012**, *4*, 2561. https://doi.org/10.1021/am300232z
32. A. K. Bansal, F. Antolini, S. Zhang, L. Stroea, L. Ortolani, M. Lanzi, E. Serra, S. Allard, U. Scherf, I. D. W. Samuel. Highly Luminescent Colloidal CdS Quantum Dots with Efficient Near-Infrared Electroluminescence in Light-Emitting Diodes. *J. Phys. Chem. C* **2016**, *120*, 1871. https://doi.org/10.1021/acs.jpcc.5b09109
33. K. E. Andersen, C. Y. Fong, W. E. Pickett. Quantum confinement in CdSe nanocrystallites. *J. Non-Cryst. Solids* **2002,** *299,* 1105. https://doi.org/10.1016/S0022-3093(01)01132-2
34. L. Meng, Q. Chen, X. Li, H. Zhang, Y Hai, Y. Yang, X. Wang, M. Luo. Enhanced Photocatalytic Nitrogen Reduction via Bismuth Nanoparticle-Decorating ZnCdS Solid Solution. *Inorg. Chem*. **2024**, *63,* 5065. https://doi.org/10.1021/acs.inorgchem.3c04566
35. W. A. A. Mohamed, H. A. E.-Gawad, S. Mekkey, H. Galal, H. Handal, H. Mousa, A. Labib. Quantum dots synthetization and future prospect applications. *Nanotechnol. Rev.* **2021**, *10,* 1926. https://doi.org/10.1515/ntrev-2021-0118
36. H. T. Tung, D. V. Thuan, J. H. Kiat, D. H. Phuc. Ag^{+} ion doped on the CdSe quantum dots for quantum dot sensitized solar cells' application. *Appl. Phys. A* **2019**, *125,* 505. https://doi.org/10.1007/s00339-019-2797-0
37. S. T. Harry, M. A. Adekanmbi. Confinement energy of Quantum dots and the Brus equation, *Int. J. Res.* **2020**, *8,* 318. https://doi.org/10.29121/granthaalayah.v8.i11.2020.2451
38. R. Köhler, W. Neumann, M. Schmidbauer, M. Hanke, D. Grigoriev, P. Schäfer, H. Kirmse, I. Häusler, R. Schneider. Structural Characterisation of Quantum Dots by X-Ray Diffraction and TEM, *Semicond*. *Nanostructures* **2008**, p. 97. https://doi.org/10.1007/978-3-540-77899-8_5
39. H. Li, H. J. Xiao, T. S. Zhu, H. C. Xuan, M. Li. Size Consideration on Shape Factor and Its Determination Role on the Thermodynamic Stability of Quantum Dots. *J. Phys. Chem. C* **2015**, *119,* 12002. https://doi.org/10.1021/acs.jpcc.5b02230
40. W. H. Qi, M. P. Wang, M. Zhou, X. Q. Shen, X. F. Zhang. Modeling cohesive energy and melting temperature of nanocrystals. *J. Phys. Chem. Solids*, 2006, 67, 851. http://dx.doi.org/10.1016/j.jpcs.2005.12.003
41. Y. Li, Y. Ding, Y. Zhang, Y. Qian. Photophysical properties of ZnS quantum dots. *J. Phys. Chem. Solids* **1999**, *60,* 13. https://doi.org/10.1016/S0022-3697(98)00247-9
42. M. A. Hegazy, A. M. Hameed. Characterization of CdSe-nanocrystals used in semiconductors for aerospace applications: Production and optical properties. *NRIAG J. Astron. Geophys* **2014**, *3,* 82. https://doi.org/10.1016/j.nrjag.2014.05.002
43. F. S. Riehle, K. Yu. Role of Alcohol in the Synthesis of CdS Quantum Dots. *Chem. Mater.* **2020**, *32,* 1780. https://doi.org/10.1021/acs.chemmater.9b04009
44. S. Bandaru, M. Palanivel, M. Ravipat, W. Y. Wu, S. Zahid, S. S. Halkarni, G. K. Dalapati, K. K. Ghosh, B. Gulyás, P. Padmanabhan, S. Chakrabortty. Highly Monodisperse, Size Tunable Glucosamine Conjugated CdSe Quantum Dots for Enhanced Cellular Uptake and Bioimaging. *ACS Omega* **2024**, *9*, 7452. https://doi.org/10.1021/acsomega.3c04962
45. W. K. Bae, K. Char, H. Hur, S. Lee. Single-Step Synthesis of Quantum Dots with Chemical Composition Gradients. *Chem. Mater.* **2008**, *20*, 531. https://doi.org/10.1021/cm070754d
46. A. R. C. Osypiw, S. Lee, S. M. Jung, S. Leoni, P. M. Smowton, B. Hou, J. M. Kim, G. A. J. Amaratunga. Solution-processed colloidal quantum dots for light emission, *Mater. Adv.* **2022**, *3*, 6773. https://doi.org/10.1039/D2MA00375A
47. B. A. A. Jahdaly, M. F. Elsadek, B.M. Ahmed, M.F. Farahat, M.M. Taher, A.M. Khalil. Outstanding Graphene Quantum Dots from Carbon Source for Biomedical and Corrosion Inhibition Applications: A Review. *Sustainability* **2021**, *13,* 2127. https://doi.org/10.3390/su13042127
48. S. Das, K. Sa, P. C Mahakul, J. Raiguru, I. Alam, B. V. R. S. Subramanyam, P. Mahanandia. Synthesis of quaternary chalcogenide CZTS nanoparticles by a hydrothermal route. *IOP Conf. Ser.: Mater. Sci. Eng.* **2018**, *338,* 012062. https://doi.org/10.1088/1757-899X/338/1/012062
49. G. B. Passos, D. V. Freitas, J. M. M. Dias, E. T. Neto, M. Navarro. One-pot electrochemical synthesis of CdTe quantum dots in cavity cell. *ElectrochimicaActa* **2016**, *190,* 689. https://doi.org/10.1016/j.electacta.2016.01.016
50. I. A. Mir, K. Das, K. Rawat, H. B. Bohidar. Hot Injection versus Room Temperature Synthesis of CdSe Quantum Dots: A Differential Spectroscopic and Bioanalyte Sensing Efficacy Evaluation. *Colloids Surf. A: Physicochem. Eng. Aspects*. **2016**, *494,* 162. https://doi.org/10.1016/j.colsurfa.2016.01.002
51. D. Mohanta, S. S. Narayanan, S. K. Pal, A. K. Raychaudhuri. Time-resolved photoluminescence decay characteristics of bovine serum albumin-conjugated semiconductor nanocrystallites. *J. Exp. Nanosci.* **2009**, *4*, 177. https://doi.org/10.1080/17458080902866204
52. A. Yakoubi, T. B. Chaabane, A. Aboulaich, R. Mahiou, L. Balan, G. Medjahdi, R. Schneider. Aqueous synthesis of Cu-doped CdZnS quantum dots with controlled and efficient photoluminescence. *J. Lumin*. **2016**, *175*, 193. https://doi.org/10.1016/j.jlumin.2016.02.035.
53. H. Zhan, P. Zhou, K. Pan, T. He, X. He, C. Zhou, Y. He, One-pot aqueous-phase synthesis of ultra-small CdSe/CdS/ CdZnS core–shell–shell quantum dots with high-luminescent efficiency and good stability. *J. Nanopart. Res.* **2013**, *15*, 1680. https://doi.org/10.1007/s11051-013-1680-8
54. K. Vidhya, M. Saravanan, G. Bhoopathi, V. P. Devarajan, S. Subanya. Structural and optical characterization of pure and starch-capped ZnO quantum dots and their photocatalytic activity. *Appl. Nanosci.* **2015**, *5,*235. https://doi.org/10.1007/s13204-014-0312-7
55. J. M. Baruah, S. Kalita, J. Narayan. Green chemistry synthesis of biocompatible ZnS quantum dots (QDs): their application as potential thin films and antibacterial agent. *Int. Nano Lett.* **2019**, *9*, 149. https://doi.org/10.1007/s40089-019-0270-x
56. Q. Zhang, Li, Y. Ma, T. Zhai. ZnSe nanostructures: Synthesis, properties and applications. *Prog. Mater. Sci.*, **2016**, *83*, 472. http://doi.org/10.1016/j.pmatsci.2016.07.005
57. S. Jagtapa, P. Chopadea, S. Tadepalli, A. Bhaleraoc, S. Gosavi. A review on the progress of ZnSe as inorganic scintillator. *Opto-Electronics Rev.* **2019**, *27*, 90. https://doi.org/10.1016/j.opelre.2019.01.001
58. U. B. Memon, U. Chatterjee, M. N. Gandhi, S. Tiwari, S. P. Duttagupta. Synthesis of ZnSe Quantum Dots with Stoichiometric Ratio Difference and Study of its Optoelectronic Property. *Procedia Mater. Sci.* **2014,** *4*, 1027. https://doi.org/10.1016/j.mspro.2014.07.393
59. P. A. Radi, A. G. Brito-Madurro, J. M. Madurro, N. O. Dantas. Characterization and properties of CdO nanocrystals incorporated in polyacrylamide. *Braz. J. Phys.* **2006**, *36,* 412. https://doi.org/10.1590/S0103-97332006000300048
60. H. Li, H. J. Xiao, T. S. Zhu, H. C. Xuan, M. Li. Size Consideration on Shape Factor and Its Determination Role on the Thermodynamic Stability of Quantum Dots. *J. Phys. Chem. C* **2015**, *119*, 12002. https://doi.org/10.1021/acs.jpcc.5b02230
61. M. Masab, H. Muhammad, F. Shah, M. Yasira, M. Hanif. Facile synthesis of CdZnS QDs: Effects of different capping agents on the photoluminescence properties.

Mater. Sci. Semicond. Process. **2018**, *81,* 113. https://doi.org/10.1016/j.mssp.2018.03.023
62. M. A. Husseina, K. A. Mohammedb, R. A. Talib. Energy band gaps and optical absorption properties of the CdZnS and CdZnS:PEO thin films prepared by chemical bath deposition. *Chalcogenide Lett.* **2022**, *19,* 239. https://doi.org/10.15251/CL.2022.195.329
63. Q. Zhang, C. Nie, C. Chang, C. Guo, X. Jin, Y. Qin, F. Li, Q. Li. Highly luminescent red emitting CdZnSe/ZnSe quantum dots synthesis and application for quantum dot light emitting diodes, *Opt. Mater. Express.* **2017**, *7,* 3875. https://doi.org/10.1364/OME.7.003875
64. W. Yue, S. Han, R. Peng, W. Shen, H. Geng, F. Wu, S. Tao, M. Wang. CuInS2 quantum dots synthesized by a solvothermal route and their application as effective electron acceptors for hybrid solar cells. *J. Mater. Chem*. **2010**, *20,* 7570. https://doi.org/10.1039/C0JM00611D
65. T. Arfin, S. Athar. Graphene for advanced organic photovoltaics, In: S. Kanchi, S. Ahmed, M.I. Sabela, C.M. Hussain (Eds.), Nanomaterials: biomedical, environmental, and engineering applications, Scrivener Publishing LLC, Beverly, **2018**, pp. 93-103. https://doi.org/10.1002/9781119370383.ch3
66. G. Chen, J. Seo, C. Yang, P. N. Prasad. Nanochemistry and nanomaterials for photovoltaics. *Chem. Soc. Rev.* **2013**, 42, 8304. https://doi.org/10.1039/C3CS60054H
67. J. H. Rhee, C. C. Chung, E. W. G. Diau. A perspective of mesoscopic solar cells based on metal chalcogenide quantum dots and organometal-halide perovskites. *NPG Asia Mater.* **2013**, *5*, 68. https://doi.org/10.1038/am.2013.53
68. S. C. Zhu, F. -X. Xiao. Transition metal chalcogenides quantum dots: emerging building blocks toward solar-to-hydrogen conversion. *ACS Catal.* **2023**, *13,* 7269. https://doi.org/10.1021/acscatal.2c05401
69. A. Qurashi. Metal Chalcogenide Nanostructures for Renewable Energy Applications, *Wiley*, **2014**, 233-246. https://doi.org/10.1002/9781119008934.ch10
70. S. Singh, Z. H. Khan, P. Kumar, M. B. Khan, P. Kumar. Quantum dots-sensitized solar cells: a review on strategic developments. *Bull. Mater. Sci.* **2022**, *45,* 81. https://doi.org/10.1007/s12034-022-02662-z
71. J. Zhu, K. Lu, J. Li, Z. Liu, W. Ma. Tandem solar cells based on quantum dots. *Mater. Chem. Front.* **2024**, *8,* 1792. https://doi.org/10.1039/D3QM01087B
72. S. R. Padmaperuma, M. Liu, R. Nakamura, Y. Tachibana. Photoinduced charge carrier dynamics of metal chalcogenide semiconductor quantum dot sensitized TiO_2 film for photovoltaic application. *J. Photopolym. Sci. Technol.* **2021**, *34,* 271. https://doi.org/10.2494/PHOTOPOLYMER.34.271
73. M. A. Mumin, K. F. Akhter, O. O. Oyeneye, W. Z. Xu, P. A. Charpentier. Supercritical Fluid Assisted Dispersion of NanoSilica encapsulated CdS/ZnS quantum dots in poly(ethylene-co-vinyl Acetate) for solar harvesting films. *ACS Appl. Nano Mater.* **2018**, *1,* 3186. https://doi.org/10.1021/acsanm.8b00390
74. P. Cui, P. K. Tamukong, S. Kilina. Effect of Binding Geometry on Charge Transfer in CdSe Nanocrystals Functionalized by N719 Dyes to Tune Energy Conversion Efficiency. *ACS Appl. Nano Mater*. **2018**, *1,* 3174. https://doi.org/10.1021/acsanm.8b00350
75. M. A. Hossain, J. R. Jennings, C. Shen, J. H. Pan, Z. Y. Koh, N. Mathews, Q. Wang. CdSe sensitized mesoscopic TiO_2 solar cells exhibiting >5% efficiency: redundancy of CdS buffer layer. *J. Mater. Chem*. **2012**, *22,* 16235. https://doi.org/10.1039/C2JM33211F
76. N. Guijarro, E. Guillén, T. Lana-Villarreal, R. Gómez. Quantum dot-sensitized solar cells based on directly adsorbed zinc copper indium sulfide colloids. *Phys. Chem. Chem. Phys*. **2014**, *16,* 9115. https://doi.org/10.1039/C4CP00294F
77. K. Zhao, Z. Pan, I. Mora-Sero, E. Canovas, H. Wang, Y. Song, X. Gong, J. Wang, M. Bonn, J. Bisquert, X. Zhong. Boosting power conversion efficiencies of quantum-dot-sensitized solar cells beyond 8% by recombination control. *J. Am. Chem. Soc*. **2015**, *137,* 5602. https://doi.org/10.1021/jacs.5b01946
78. J. Yang and X. Zhong. CdTe based quantum dot sensitized solar cells with efficiency exceeding 7% fabricated from quantum dots prepared in aqueous media. *J. Mater. Chem. A* **2016**, *4,* 16553. https://doi.org/10.1039/C6TA07399A
79. A. Arivarasan, S. Bharathi, V. Vijayaraj, G. Sasikala, R. Jayavel. Evaluation of reaction parameters dependent optical properties and its photovoltaics performance of CdTe QDs. J. *Inorg. Organomet. Polym. Mater*. **2018**, *28,* 1263. https://doi.org/10.1007/s10904-018-0803-1
80. G. Shen, Z. Du, Z. Pan, J. Du, X. Zhong. Solar paint from TiO_2 particles supported quantum dots for photoanodes in quantum dot-sensitized solar cells. *ACS Omega* **2018**, *3,* 1102. https://doi.org/10.1021/acsomega.7b01761
81. H. Zhang, W. Fang, W. Wang, N. Qian, X. Ji. Highly efficient Zn-Cu-In-Se quantum dot-sensitized solar cells through surface capping with ascorbic acid. *ACS Appl. Mater. Interfaces* **2019**, *11,* 6927. https://doi.org/10.1021/acsami.8b18033
82. B. Fu, C. Deng, L. Yang. Efficiency enhancement of solid-state CuInS2 quantum dot-sensitized solar cells by improving the charge recombination. *Nanoscale Res*. *Lett.* **2019**, *14,* 198. https://doi.org/10.1186/s11671-019-2998-7
83. P. Xu, X. Chang, R. Liu, L. Wang, X. Li, X. Zhang, X. Yang, D. Wang, W. Lu. Boosting power conversion efficiency of quantum dot-sensitized solar cells by integrating concentrating photovoltaic concept with double photoanodes. *Nanoscale Res. Lett.* **2020**, *15,* 188. https://doi.org/10.1186/s11671-020-03424-8
84. Y. Lin, H. Song, J. Zhang, H. Rao, Z. Pan, X. Zhong. Hole transport materials mediating hole transfer for high efficiency quantum dot sensitized solar cells. *J. Mater. Chem. A* **2021**, *9,* 997. https://doi.org/10.1039/D0TA10702F
85. H. Song, Y. Lin, M. Zhou, H. Rao, Z. Pan, X. Zhong. Zn–Cu– In–S–Se quinary "green" alloyed quantum-dot-sensitized solar cells with a certified effciency of 14.4%. *Angew. Chem. Int. Ed.* **2020**, *60,* 6137. https://doi.org/10.1002/anie.202014723
86. E. Elibol. Quantum dot sensitized solar cell design with surface passivized CdSeTe QDs. *Sol. Energy* **2020**, *206,* 741. https://doi.org/10.1016/j.solener.2020.06.002
87. G. Konstantatos, E. H. Sargent. Nanostructured materials for photon detection. *Nat. Nanotechnol.* **2010**, *5,* 391. https://doi.org/10.1038/nnano.2010.78
88. H. Tang, J. Zhong, W. Chen, K. Shi, G. Mei, Y. Zhang, Z. Wen, P. Müller-Buschbaum, D. Wu, K. Wang, X. W. Sun. Lead Sulfide Quantum Dot Photodetector with Enhanced Responsivity through a Two-Step Ligand-Exchange Method. *ACS Appl. Nano Mater.* **2019**, *2,* 6135. https://doi.org/10.1021/acsanm.9b00889
89. B. Cook, M. Gong, D. Ewing, M. Casper, A. Stramel, A. Elliot, J. Wu. Inkjet Printing Multicolor Pixelated QDs on Graphene for Broadband Photodetection. *ACS Appl. Nano Mater.* **2019**, *2,* 3246. https://doi.org/10.1021/acsanm.9b00539
90. N. Mahmoud, W. Walravens, J. Kuhs, C. Detavernier, Z. Hens, G. Roelkens. Micro-Transfer-Printing of Al_2O_3-Capped Short Wave-Infrared PbS Quantum Dot Photoconductors. *ACS Appl. Nano Mater*. **2019**, *2.* 299. https://doi.org/10.1021/acsanm.8b01915
91. B. Hafiz, M. R. Scimeca, P. Zhao, I. J. Paredes, A. Sahu, D. K. Ko. Silver Selenide Colloidal QDs for Mid Wavelength Infrared Photodetection. *ACS Appl. Nano Mater.* **2019**, *2,* 1631. https://doi.org/10.1021/acsanm.9b00069

92. A. Paliwal, S. V. Singh, A. Sharma, A. Sugathan, S. W. Liu, S. Biring, B. N. Pal. Microwave-Polyol Synthesis of Sub-10-nm PbS Nanocrystals for Metal Oxide/Nanocrystal Heterojunction Photodetectors. *ACS Appl. Nano Mater*. **2018**, *1,* 6063. https://doi.org/10.1021/acsanm.8b01194
93. E. Lhuillier, P. Guyot-Sionnest. Recent Progresses in Mid Infrared Nanocrystal Optoelectronics. IEEE *J. Sel. Top. Quantum Electron.* **2017**, *23,* 6000208. https://doi.org/10.1109/JSTQE.2017.2690838
94. X. Lyu. Recent Progress on Infrared Detectors: Materials and Applications. *HSET* **2022**, *27,* 191. https://doi.org/10.54097/hset.v27i.3747
95. J. Chen, J. Chen, X. Li, J. He, L. Yang, J. Wang, F. Yu, Z. Zhao, C. Shen, H. Guo, L. Guanhai, X. Chen, W. Lu. High-performance HgCdTe avalanche photodetector enabled with suppression of band-to-band tunneling effect in mid-wavelength infrared. *NPJ Quantum Mater*. **2021**, *6,* 2397. https://doi.org/10.1038/s41535-021-00409-3
96. L. Ciura, M. Kopytko, P. Martyniuk. Low-frequency noise limitations of InAsSb-, and HgCdTe-based infrared detectors. *Sens. Actuators A Phys*. **2020**, *305,* 111908. https://doi.org/10.1016/j.sna.2020.111908
97. K. Batty, I. Steele, C. Copperwheat. Laboratory and On-sky Testing of an InGaAs Detector for Infrared Imaging. *Publ. Astron. Soc. Pac*. **2022**, *134,* 65001. https://doi.org/10.1088/1538-3873/ac71cc.
98. X. Zhao, H. Ma, H. Cai, Z. Wei, Y. Bi, X. Tang, T. Qin. Lead chalcogenide colloidal QDs for infrared photodetectors. *Materials* **2023**, *16,* 5790. https://doi.org/10.3390/ma16175790.
99. Q. Hao, H. Ma, X. Xing, X. Tang, Z. Wei, X. Zhao, M. Chen. Mercury Chalcogenide colloidal quantum dots for infrared photodetectors. *Material* **2023**, *16,* 7321. https://doi.org/10.3390/ma16237321
100. Y. Tian, H. Luo, M. Chen, C. Li, S. V. Kershaw, R. Zhang, A. L. Rogach. Mercury chalcogenide colloidal QDsfor infrared photodetection: from synthesis to device applications. *Nanoscale* **2023**, *15,* 6476. https://doi.org/10.1039/D2NR07309A
101. P. Zhao, T. Qin, G. Mu, S. Zhang, Y. Luo, M. Chen, X. Tang. Band-engineered dual-band visible and short infrared photodetector with metal chalcogenide colloidal quantum dots. *J. Mater. Chem. C* **2023**, *11,* 2842. https://doi.org/10.1039/D3TC00066D
102. A. Maimulyanti, A. R. Prihadi, B. Mellisani, I. Nurhidayati, F. A. Rachmawati Putri, F. Puspita, R. W. Widarsih. Green Extraction Technique to Separate Tannin from Coffee Husk Waste Using Natural Deep Eutectic Solvent (NADES). *Rasayan J. Chem*. **2023,** *16*, 2239. http://dx.doi.org/10.31788/RJC.2023.1638334
103. R. Bushra, T. Arfin, M. Oves, W. Raza, F. Mohammad, M. A. Khan, A. Ahmed, A. Azam, M. Muneer. Development of PANI/MWCNTs decorated with cobalt oxide nanoparticles toward multiple electrochemical, photocatalytic and biomedical application sites. *New J. Chem*. **2016**, *40,* 9448. https://doi.org/10.1039/C6NJ02054B
104. Y. -H. Liu, C. -L. Yang, M. -S. Wang, X. -G. Ma, Y. -G. Yi. Ternary chalcogenides $XGsS_2$ (X = Ag or Cu) for photocatalytic hydrogen generation from water splitting under irradiation of visible light. *Int. J. Quantum Chem*. **2020**, *120,* 26166. https://doi.org/10.1002/qua.26166
105. C. Kumari, P. Sharma, S. Chhoker. Photocatalytic activity of quaternary chalcogenide for methylene blue degradation. *AIP Conf. Proc.* **2024**, *2995,* 020066. https://doi.org/10.1063/5.0177995
106. J. A. Caputo, L. C. Frenette, N. Zhao, K. L. Sowers, T. D. Krauss, D. J. Weix. General and Efficient C-C Bond Forming Photoredox Catalysis with Semiconductor Quantum Dots. *J. Am. Chem. Soc*. **2017**, *139,* 4250. https://doi.org/10.1021/jacs.6b13379
107. Z. Zhang, K. Edme, S. Lian, E. A. Weiss. Enhancing the Rate of Quantum-Dot-Photocatalyzed Carbon-Carbon Coupling by Tuning the Composition of the Dot's Ligand Shell. *J. Am. Chem. Soc.* **2017**, *139,* 4246. https://doi.org/10.1021/jacs.6b13220
108. Y. Zhou, S. Yang, D. Fan, J. Reilly, H. Zhang, W. Yao, J. Huang. Carbon Quantum Dot/TiO_2 Nanohybrids: Efficient Photocatalysts for Hydrogen Generation via Intimate Contact and Efficient Charge Separation. *ACS Appl. Nano Mater*. **2019**, *2,* 1027. https://doi.org/10,1021/acsanm.8b02310
109. A. Samanta, J. C. Breger, K. Susumu, E. Oh, S. A. Walper, N. Bassim, I. L. Medintz. DNA-Nanoparticle Composites Synergistically Enhance Organophosphate Hydrolase Enzymatic Activity. *ACS Appl. Nano Mater*. **2018**, *1,* 3091. https://pubs.acs.org/doi/abs/10.1021/acsanm.8b00933
110. E. G. Durmusoglu, Y. Turker, H. Y. Acar. Luminescent PbS and PbS/CdS QDs with Hybrid Coatings as Nanotags for Authentication of Petroleum Products. *ACS Appl. Nano Mater*. **2019**, *2,* 7737. https://doi.org/10.1021/acsanm.9b01780
111. F. M. de Melo, D. Grasseschi, B. B. N. S. Brandao, Y. Fu, H. E. Toma. Superparamagnetic Maghemite-Based CdTe quantum dots as Efficient Hybrid Nanoprobes for Water-Bath Magnetic Particle Inspection. *ACS Appl. Nano Mater*. **2018**, *1,* 2858. https://doi.org/10.1021/acsanm.8b00502
112. L. Meng, Q. Chen, X. Li, H. Zhang, Y. Hai, Y. Hai, Y. Yang, X. Wang, and M. Luo. Enhanced photocatalytic nitrogen reduction via bismuth nanoparticle-decorating ZnCdS solid solution. *Inorg. Chem*. **2024**, *63,* 5065. https://doi.org/10.1021/acs.inorgchem.3c04566
113. L. Sun, J. J. Choi, D. Stachnik, A. C. Bartnik, B. R. Hyun, G. G. Malliaras, T. Hanrath, F. W. Wise. Bright infrared quantum-dot light-emitting diodes through inter-dot spacing control. *Nature Nanotech.* **2012**, *7,* 369. https://doi.org/10.1038/nnano.2012.63
114. X. Yang, F. Ren, Y. Wang, T. Ding, H. Sun, D. Ma, X. W. Sun. Iodide capped PbS/CdS core-shell QDs for efficient long-wavelength near-infrared light-emitting diodes. *Sci. Rep.* **2017**, *7,* 14741. https://doi.org/10.1038/s41598-017-15244-5.
115. X. Gong, Z. Yang, G. Walters, R. Comin, Z. Ning, E. Beauregard, V. Adinolfi, O. Voznyy, E. H. Sargent. Highly efficient quantum dot near-infrared light-emitting diodes. *Nat. Photonics* **2016**, *10,* 253. https://doi.org/10.1038/nphoton.2016.11
116. S. Pradhan, F. D. Stasio, Y. Bi, S. Gupta, S. Christodoulou, A. Stavrinadis, G. Konstantatos. High-efficiency colloidal quantum dot infrared light-emitting diodes via engineering at the supra-nanocrystalline level. *Nat. Nanotech*. **2019**, *14,* 72. https://doi.org/10.1038/s41565-018-0312-y
117. G. J. Supran, K. W. Song, G. W. Hwang, R. E. Correa, J. Scherer, E. A. Dauler, Y. Shirasaki, M. G. Bawendi, V. Bulović. High-performance shortwave-infrared light-emitting devices using core-shell (PbS-CdS) colloidal quantum dots. *Adv. Mater.* **2015**, *27,* 1437. https://doi.org/10.1002/adma.201404636
118. X. Dai, Z. Zhang, Y. Jin, Y. Niu, H. Cao, X. Liang, L. Chen, J. Wang, X. Peng. Solution-processed, high-performance light-emitting diodes based on quantum dots. *Nature* **2014**, *515,* 96. https://doi.org/10.1038/nature13829
119. H. -M. Kim, D. Geng, J. Kim, E. Hwang, J. Jang. Metal-Oxide stacked electron transport layer for highly efficient inverted quantum-dot light emitting diodes. *ACS Appl. Mater.* **2016**, *8*, 28727. https://doi.org/10.1021/acsami.6b10314
120. B. Mahler, N. Lequeux, B. Dubertret. Ligand-controlled polytypism of thick-shell CdSe/CdS nanocrystals. *J. Am. Chem. Soc.* **2010**, *132,* 953. https://doi.org/10.1021/ja9034973
121. B. Chon, S. J. Lim, W. Kim, J. Seo, H. Kang, T. Joo, J. Hwang, S. K. Shin. Shell and ligand-dependent blinking of

CdSe-based core/shell nanocrystals. *Phys. Chem. Chem. Phys.* **2010**, *12,* 9312. https://doi.org/10.1039/B924917F
122. B. N. Pal, Y. Ghosh, S. Brovelli, R. Laocharoensuk, V. I. Klimov, J. A. Hollingsworth, H. Htoon., Giant CdSe/CdS core/shell nanocrystal QDs as efficient electroluminescent materials: strong influence of shell thickness on light-emitting diode performance. *Nano Lett*. **2012**, *12,* 331. https://doi.org/10.1021/nl203620f
123. O. Chen, J. Zhao, V. P. Chauhan, J. Cui, C. Wong, D. K. Harris, H. Wei, H. S. Han, D. Fukumura, R. K. Jain and M. G. Bawendi. Compact high-quality CdSe/CdS core/shell nanocrystals with narrow emission linewidths and suppressed blinking. *Nat. Mater*. **2013**, *12,* 445. https://doi.org/10.1038/nmat3539
124. C. Pu, X. Dai, Y. Shu, M. Zhu, Y. Deng, Y. Jin, X. Peng. Electrochemically-stable ligands bridge the photoluminescence-electroluminescence gap of quantum dots. *Nat. Commun.* **2020**, *11,* 937. https://doi.org/10.1038/s41467-020-14756-5
125. S. Kim, J.-A. Kim, T. Kim, H. Chung, S. Park, S.-M. Choi, H.-M. Kim, D.-Y. Chung, E. Jang. Efficient blue-light-emitting Cd-free colloidal quantum well and its application in electroluminescent devices. *Chem. Mater*. **2020**, *32,* 5200. https://doi.org/10.1021/acs.chemmater.0c01275
126. J. Jiang, S. Zhang, Q. Shan, L. Yang, J. Ren, Y. Wang, S. Jeon, H. Xiang, H. Zeng. High-color-rendition white QLEDs by balancing red, green, and blue centres in eco-friendly ZnCuGaS:In@ZnS quantum dots. *Adv. Mater*. **2024**, *36*. e2304772. https://doi.org/10.1002/adma.202304772
127. S. Zhou, Y. Ma, X. Zhang, W. Lan, X. Yu, B. Xie, K. Wang, X. Luo. White-Light-Emitting Diodes from Directional Heat-Conducting Hexagonal Boron Nitride Quantum Dots. *ACS Appl. Nano Mater.* **2020**, *3,* 814. https://doi.org/10.1021/acsanm.9b02321
128. J. Choi, W. Choi, D. Y. Jeon. Ligand-Exchange-Ready CuInS2/ZnS QDs via Surface-Ligand Composition Control for Film-Type Display Devices. *ACS Appl. Nano Mater*. **2019**, *2,* 5504. https://doi.org/10.1021/acsanm.9b01085
129. T. Afrin, S. Fatma. Anticipating behavior of advanced materials in healthcare, In: A. Tiwari, A.N. Nordin (Eds.), *Advanced biomaterials and biodevices*, Scrivener Publishing LLC, Beverly, **2014**, pp. 243-287. https://doi.org/10.1002/9781118774052.ch7
130. W. Su, D. Yang, Y. Kong, W. Zhang, J. Wang, Y. Fei, R. Guo, J. Ma, L. Mi. AgInS2/ZnS QDsfor noninvasive cervical cancer screening with intracellular pH sensing using fluorescence lifetime imaging microscopy. *Nano Res.* **2022**, *15,* 5193. https://doi.org/10.1007/s12274-022-4104-1
131. Z. Piao, D. Yang, Z. Cui, H. He. S. Mei, H. Lu, Z. Fu, L. Wang, W. Zhang, R. Guo. Recent advances in metal chalcogenide quantum dots: from material design to biomedical applications. *Adv. Funct. Mater.* **2022**, 32, 2207662. https://doi.org/10.1002/adfm.202207662
132. X. Wu, H. Liu, J. Liu, K. N. Haley, J. A. Treadway, J. P. Larson, N. Ge, F. Peale, M. P. Bruchez. Immunofluorescent labeling of cancer marker her2 and other cellular targets with semiconductor quantum dots. *Nat. Biotechnol*. **2003**, *21,* 41. https://doi.org/10.1038/nbt764
133. S. Mallick, P. Kumar, A. L. Koner. Freeze-Resistant Cadmium-Free QDsfor Live-Cell Imaging. *ACS Appl. Nano Mater.* **2019**, *2,* 661. https://doi.org/10.1021/acsanm.8b02231
134. A. T. Nguyen, D. R. Baucom, Y. Wang, C. D. Heyes. Compact, fast blinking Cd-free QDsfor super-resolution fluorescence imaging. *Chem. Biomed. Imaging* **2023**, *1,* 251. https://doi.org/10.1021/cbmi.3c00018
135. Y. Li, P. Zhang, W. Tang, K. J. Mchugh, S. V. Kershaw, M. Jiao, X. Huang, S. Kalytchuk, C. F. Perkinson, S. Yue, Y. Qiao, L. Jing, M. Gao, B. Han. Bright, magnetic NIR-II quantum dot probe for sensitive dual-modality imaging and intensive combination therapy of cancer. *ACS Nano* **2022**, *16,* 8076. https://doi.org/10.1021/acsnano.2c01153
136. H. Xue, J. Zhao, Q. Zhou, D. Pan, Y. Zhang, Y. Zhang, Y. Shen. Boosting the Sensitivity of a Photoelectrochemical Immunoassay by Using SiO2@polydopamine Core-Shell Nanoparticles as a Highly Efficient Quencher. *ACS Appl. Nano Mater.* **2019**, *2,* 1579. https://doi.org/10.1021/acsanm.9b00050
137. M. Freitas, M. M. P. S. Neves, H. P. A. Nouws, C. Delerue-Matos. Quantum dots as nanolabels for breast cancer biomarker HER2-ECD analysis in human serum. *Talanta* **2020**, *208,* 120430. https//doi.org/10.1016/j.talanta.2019.120430
138. M. Freitas, H. P. A. Nouws, E. Keating, V. C. Fernandes, C. Delerue-Matos. Immunomagnetic bead-based bioassay for the voltammetric analysis of the breast cancer biomarker HER2-ECD and tumor cells using QDsas detection labels. *Mikrochim. Acta* **2020**, *187,* 184. https://doi.org/ 10.1007/s00604-020-4156-4
139. S. A. Diaz, G. Lasarte-Aragones, R. G. Lowery, Aniket, J. N. Vranish, W. P. Klein, K. Susumu, I. L. Medintz. Quantum dots as Forster Resonance Energy Transfer Acceptors of Lanthanides in Time-Resolved Bioassays. *ACS Appl. Nano Mater.* **2018**, *1*, 3006. https://doi.org/10.1021/acsanm.8b00613
140. D. N. Williams, S. Pramanik, R. P. Brown, B. Zhi, E. McIntire, N. V. Hudson-Smith, C. L. Haynes, Z. Rosenzweig. Adverse interactions of luminescent semiconductor quantum dots with liposomes and shewanella oneidensis. *ACS Appl. Nano Mater.* **2018,** *1,* 4788. https://doi.org/10.1021/acsanm.8b01000
141. G. Lv, W. Guo, W. Zhang, T. Zhang, S. Li, S. Chen, A. S. Eltahan, D. Wang, Y. Wang, J. Zhang, P. C. Wang, J. Chang, X. -J. Liang. Near-infrared emission CuInS/ZnS quantum dots: all-in-one theranostic nanomedicines with intrinsic fluorescence/photocoustic imaging for tumor phototherapy. *ACS Nano* **2016**, *10,* 9637. https://doi.org/10.1021/acsnano.6b05419
142. V. K. Singh, H. Mishra, R. Ali, S. Umrao, R. Srivastava, S. Abraham, A. Misra, V. N. Singh, H. Mishra, R. S. Tiwari, A. Srivastava. In situ functionalized fluorescent WS_2-QDs as sensitive and selective probe for Fe^{3+} and a detailed study of its fluorescence quenching. *ACS Appl. Nano Mater*. **2019**, *2,* 566. https://doi.org/10.1021/acsanm.8b02162
143. S. R. Ahmed, J. Cirone, A. Chen. Fluorescent Fe_3O_4 quantum dots for H_2O_2 detection. *ACS Appl. Nano Mater*. **2019**, *2,* 2076. https://doi.org/10.1021/acsanm.9b00071
144. C. Wei, X. Wei, Z. Hu, D. Yang, S. Mei, G. Zhang, D. Su, W. Zhang, R. Guo. A fluorescent probe for Cd^{2+} detection based on the aggregation-induced emission enhancement of aqueous Zn-Ag-In-S quantum dots. *Anal. Methods* **2019**, *11,* 2559. https://doi.org/10.1039/C9AY00716D
145. C. C. Hewa-Rahinduwage, X. Geng, K. L. Silva, X. Niu, L. Zhang, S. L. Brock, L. Luo. Reversible electrochemical gelation of metal chalcogenide quantum dots. *J. Am. Chem. Soc.* **2020**, *142,* 12207. https://doi.org/10.1021/jacs.0c03156
146. A. Mirzaei, Z. Kordrostami, M. Shahbaz, J. Y. Kim, H. W. Kim. Resistive-based gas sensors using quantum dots: a review. *Sensors* **2022**, *22,* 4369. https://doi.org/10.3390/s22124369
147. X. Geng, X. Liu, L. Mawella-Vithanage, C. C. Hewa-Rahinduwage, L. Zhang, S. L. Brock, T. Tan, L. Luo. Photoexcited NO_2 enables accelerated response and recovery kinetics in light-activated NO_2 gas sensing. *ACS Sens.* **2021**, *6,* 4389. https://doi.org/10.1021/acssensors.1c01694
148. T. Jiang, X. Liu, J. Sun. UV-enhanced NO_2 sensor using ZnO QDs sensitized SnO_2 porous nanowires. *Nanotechnology* **2022**, *33,* 185501. https://doi.org/10.1088/1361-6528/ac49c1

149. Q. Lin, F. Zhang, N. Zhao, L. Zhao, Z. Wang, P. Yang, D. Lu, T. Dong, Z. Jiang. A flexible and wearable nylon fiber sensor modified by reduced graphene oxide and ZnO QDs for wide-range NO_2 gas detection at room temperature. *Materials* **2022,** *15,* 3772. https://doi.org/10.3390/ma15113772
150. Y. Liu, H. Wang, K. Chen, T. Yang, S. Yang, W. Chen. Acidic site-assisted ammonia sensing of novel $CuSbS_2$ quantum dots/reduced graphene oxide composites with an ultralow detection limit at room temperature. *ACS Appl. Mater. Interfaces* **2019**, *11,* 9573. https://doi.org/10.1021/acsami.8b20830
151. I. Sharma, K. N. Kumar, J. Choi. Highly sensitive chemiresistive detection of NH_3 by formation of WS_2 nanosheet and SnO_2 quantum dot heterostructures. *Sensors Actuators B Chem.* **2023**, *375,* 132899. https://doi.org/10.1016/j.snb.2022.132899
152. K. Rathi, K. Pal. Ruthenium-decorated tungsten disulfide quantum dots for a CO_2 gas sensor. *Nanotechnology* **2020,** *31,* 135502. https://doi.org/10.1088/1361-6528/ab5cd3
153. B. Bertrand, S. Hermelin, S. Takada, M. Yamamoto, S. Tarucha, A. Ludwig, A. D. Wieck, C. Bäuerle, T. Meunier. Fast spin information transfer between distant quantum dots using individual electrons, *Nature Nanotech.* **2016**, *11,* 672. https://doi.org/10.1038/nnano.2016.82
154. L. Pavesi, L D Negro, C Mazzoleni, G Franzo, F Priolo. Optical gain in silicon nanocrystals. *Nature.* **2000**, *408,* 440.https://doi.org/10.1038/35044012
155. Y. J. Jeong, D. -J. Yun, S. H. Noh, C. E. Park, J. Jang. Surface modification of CdSe quantum-dot floating gates for advancing light-erasable organic field-effect transistor memories. *ACS Nano*. **2018**, *12,* 7701. https://doi.org/10.1021/acsnano.8b01413
156. Y. Wu, Y. Wei, Y. Huang, F. Cao, D. Yu, X. Li, H. Zeng. Capping $CsPbBr_3$ with ZnO to improve performance and stability of perovskite memristors. *Nano Res.* **2017**, *10,* 1584. https://doi.org/10.1007/s12274-016-1288-2
157. S. R Bauers, M. B. Tellekamp, D. M Roberts, B. Hammett, S. Lany, A. J Ferguson, A. Zakutayev, S. U Nanoyakkara. Metal chalcogenides for neuromorphic computing: emerging materials and mechanisms. *Nanotechnology* **2021**, *32,* 372001. https://doi.org/10.1088/1361-6528/abfa51
158. K. C. Kwon, J. H. Baek, K. Hong, S. Y. Kim, H. W. Jang. Memristive devices based on two- dimensional transition metal chalcogenides for neuromorphic computing. *Nano-micro Lett.* **2022**, *14,* 58. https://doi.org/10.1007/s40820-021-00784-3
159. G. Cao, P. Meng, J. Chen, H. Liu, R. Bian, C. Zhu, F. Liu, Z. Liu. 2D material based synaptic devices for neuromorphic computing. *Adv. Funct. Mater.* **2020**, *31,* 2005443. https://doi.org/10.1002/adfm.202005443
160. M. Xu, X. Mai, J. Lin, W. Zhang, Y. Li, Y. He, H. Tong, X. Hou, P. Zhou, X. Miao. Recent advances on neuromorphic devices based on chalcogenide phase-change materials. *Adv. Funct. Mater.* **2020**, *30,* 2003419. https://doi.org/10.1002/adfm.202003419
161. Z. Lv, Y. Wang, J. Chen, J. Wang, Y. Zhou, S. -T. Han. Semiconductor quantum dots for memories and neuromorphic computing systems. *Chem. Rev***. 2020**, *120,* 3941.https://doi.org/10.1021/acs.chemrev.9b00730